

**P_1 -NONCONFORMING QUADRILATERAL FINITE ELEMENT
SPACE WITH PERIODIC BOUNDARY CONDITIONS:
PART I. FUNDAMENTAL RESULTS ON DIMENSIONS, BASES,
SOLVERS, AND ERROR ANALYSIS**

JAERYUN YIM* AND DONGWOO SHEEN †

Abstract. The P_1 -nonconforming quadrilateral finite element space with periodic boundary condition is investigated. The dimension and basis for the space are characterized with the concept of minimally essential discrete boundary conditions. We show that the situation is totally different based on the parity of the number of discretization on coordinates. Based on the analysis on the space, we propose several numerical schemes for elliptic problems with periodic boundary condition. Some of these numerical schemes are related with solving a linear equation consisting of a non-invertible matrix. By courtesy of the Drazin inverse, the existence of corresponding numerical solutions is guaranteed. The theoretical relation between the numerical solutions is derived, and it is confirmed by numerical results. Finally, the extension to the three dimensional is provided.

Key words. Finite element method, nonconforming, periodic boundary condition.

AMS subject classifications. 65N30

1. Introduction. Many macroscopic material properties are obtained from the knowledge of accurate microscopic material properties. However in most realistic cases the ratio of macro scale to micro scale is so large that it cannot be directly computed the dynamics described at the microscale level. Therefore usually upscaling techniques are used to reduce the micro scale level computation to approximately obtain macroscopic properties. Recently, several efficient multiscale methods have been developed towards that direction. These include numerical homogenization [4, 5, 13, 14], MsFEM (multiscale finite element methods) and GMsFEM (generalized MsFEM) [12, 10, 11, 17], VMS (variational multiscale finite element methods) [18], MsFVM (multiscale finite volume methods) [20] and HMM (heterogeneous multiscale methods) [1, 9]. In numerical homogenization and upscaling of multiscale problems one often needs to solve periodic boundary value problems at microscale level efficiently.

The P_1 -nonconforming quadrilateral finite element [27] has an advantage in computing stiffness matrix as the gradient of linear polynomials is constant in each quadrilateral as well as it has the smallest number of DOFs (degrees of freedom) for given quadrilateral mesh. There have been a number of studies about this finite element for fluid dynamics, elasticity, electromagnetics [23, 15, 25, 24, 26, 28, 8, 16]. Unlikely other finite elements, this space is strongly tied with the boundary condition for given problem due to the dice rule constraint element by element (See (3.1)). Most of those works are focused on the finite element space with Dirichlet and/or Neumann BCs. Altmann and Carstensen [2] show the dimension of, and a basis for the finite element space with inhomogeneous Dirichlet BCs which shares similar discrete nature with the Neumann boundary case.

On the other hand, the P_1 -nonconforming quadrilateral element space with periodic BC has not been investigated. Thus, it is our intention to investigate its dimension and basis with periodic BC.

*Interdisciplinary Program in Computational Science & Technology, Seoul National University, Seoul 08826, Korea; *current address*: Encored Technologies, 215 Bongeunsa-ro, Gangnam-gu, Seoul 06109, Korea. jaeryun.yim@gmail.com

†Department of Mathematics, Seoul National University, Seoul 08826, Korea. sheen@snu.ac.kr

The discrete formulation of periodic problems yields singular linear systems, which can be dealt with various kinds of generalized inverses of a matrix. Among them, we will concentrate on the Drazin inverse, as it can be expressed as a matrix polynomial, since the Krylov method, which is based on the same idea on matrix polynomials, can be applied to singular linear systems. One of the most important properties of the Drazin inverse is the expressibility it as a polynomial in the given matrix. The Krylov iterative method for a nonsingular linear system is established on this property. The Krylov scheme can be applied to a singular linear system as well under proper consistency conditions [19, 22, 30, 7, 3, 6].

The aim of this paper is to investigate the structure of the P_1 -nonconforming quadrilateral finite element spaces with periodic BC thoroughly and to suggest some iterative methods to solve the resulting linear systems based on the idea of Drazin inverse. An application for nonconforming heterogeneous multiscale methods (NcHMM) of P_1 -nonconforming quadrilateral finite element will appear in [29].

The organization of the paper is as follows. In Section 2, we give a brief explanation for the P_1 -nonconforming quadrilateral finite element and the Drazin inverse. We investigate the dimension of the finite element spaces with various BCs, including periodic condition which is our main concern, in Section 3. We introduce the concept of *minimally essential discrete BCs* to analyze the precise effects of given BC on the dimension of the corresponding finite element space. In Section 4, a basis for the periodic nonconforming finite element space is constructed. It consists of node-based functions by identifying boundary node-based functions in a suitable way and a complementary basis consisting of a few alternating functions is considered. We propose several numerical schemes for solving a second-order elliptic problem with periodic BC in Section 5. We use an efficient iterative method based on the Krylov space in help of the Drazin inverse of the corresponding singular matrix. The relationship between solutions of the schemes will be discussed. Finally, we extend all our results to the 3D case in Section 6.

2. Preliminaries and notations. In this section some basics on the Drazin inverse and the P_1 -nonconforming quadrilateral finite element will be briefly reviewed. Also notations to be used are described.

2.1. The Drazin inverse. Let A be a linear transformation on \mathbb{C}^n . The *index* of A , denoted by $\text{Ind}(A)$, is defined as the smallest nonnegative integer k such that

$$\text{Im } A^0 \supset \text{Im } A \supset \cdots \supset \text{Im } A^{k-1} \supset \text{Im } A^k = \text{Im } A^{k+1} = \cdots ,$$

or equivalently

$$\ker A^0 \subset \ker A \subset \cdots \subset \ker A^{k-1} \subset \ker A^k = \ker A^{k+1} = \cdots .$$

It yields that, restricted on $\text{Im } A^k$, the transformation A becomes an invertible linear transformation. The Drazin inverse of A , denoted by A^D , is defined as follows: for $u = v + w \in \mathbb{C}^n$ where $v \in \text{Im } A^k$ and $w \in \ker A^k$, $A^D u := A|_{\text{Im } A^k}^{-1} v$. One of the most important properties of the Drazin inverse matrix of A is that it is expressible as a polynomial in A :

THEOREM 2.1 ([7]). *If $A \in \mathbb{C}^{n \times n}$, then there exists a polynomial $p(x)$ such that $A^D = p(A)$.*

For a singular matrix A , a unique Drazin inverse solution can be found by using the Krylov iterative method under some proper consistency conditions. For details, see [7, 19].

THEOREM 2.2 ([19]). *Let m be the degree of the minimal polynomial for A , and let k be the index of A . If $b \in \text{Im } A^k$, then the linear system $Ax = b$ has a unique Krylov solution $x = A^D b \in \mathcal{K}_{m-k}(A, b)$. If $b \notin \text{Im } A^k$, then $Ax = b$ does not have a solution in the Krylov space $\mathcal{K}_n(A, b)$.*

2.2. Notations. For $d = 2$ or 3 , let $\Omega = \prod_{j=1}^d (0, \ell_j) \subset \mathbb{R}^d$ denote a d -dimensional rectangular domain. Let $(\mathcal{T}_h)_{0 < h < \min_{j=1}^d (\ell_j)}$ be the quasiuniform family of triangulations of Ω into d -dimensional polyhedral subdomains Q_h 's which are convex and topologically equivalent to d -dimensional cubes, with maximum diameter bounded by the mesh parameter h . We further assume that, for $0 < h < \min_{j=1}^d (\ell_j)$, \mathcal{T}_h is topologically and combinatorially equivalent to the $N_{x_1} \times \cdots \times N_{x_d}$ uniform d -dimensional rectangular decomposition, say $\tilde{\mathcal{T}}_h$. We will call that the sequences of elements, faces, and vertices in \mathcal{T}_h are aligned in the *topological x_k -direction* we mean they are images of elements, faces, and vertices in $\tilde{\mathcal{T}}_h$ aligned in the x_k -direction.

Let \mathcal{F}_h , \mathcal{F}_h^i , \mathcal{F}_h^b , and $\mathcal{F}_h^{b,opp}$ denote the sets of all $(d-1)$ -dimensional faces, interior faces, boundary faces, and boundary face pairs on opposite boundary position, respectively. Let \mathcal{N}_h denote the set of all nodes in \mathcal{T}_h . For periodic BC, we assume that for each h , \mathcal{T}_h is decomposed such that the periodically opposite boundary pairs in $\mathcal{F}_h^{b,opp}$ are congruent.

From now on, for each face f , let $\sigma_f^{(\iota)}$, $\iota = i, m$, denote the functionals which take the face average value and the midpoint value at the face midpoint m_f , respectively, such that $\sigma_f^{(i)}(u) = \frac{1}{|f|} \int_f u \, ds$ and $\sigma_f^{(m)}(u) = u(m_f)$ for given function u . We adopt several standard Sobolev spaces and discrete function spaces for the P_1 -nonconforming quadrilateral finite element:

$C_{\#}^{\infty}(\Omega)$ = the subset of $C^{\infty}(\mathbb{R}^d)$ of Ω -periodic functions restricted to Ω ,

$$H_{\#}^1(\Omega) = \overline{C_{\#}^{\infty}(\Omega)}^{H^1(\Omega)}, \quad H_{\#}^1(\Omega)/\mathbb{R} = \{v \in H_{\#}^1(\Omega) \mid \int_{\Omega} v = 0\},$$

$$V^h = \{v_h \in L^2(\Omega) \mid v_h|_K \in \mathcal{P}_1(K) \forall K \in \mathcal{T}_h, \sigma_f^{(i)}([v_h]_f) = 0 \forall f \in \mathcal{F}_h^i\},$$

$$V_0^h = \{v_h \in V^h \mid \sigma_f^{(i)}(v_h) = 0 \forall f \in \mathcal{F}_h^b\}, \quad V_{\#}^h = \{v_h \in V^h \mid \sigma_{f_1}^{(i)}(v_h) = \sigma_{f_2}^{(i)}(v_h) \\ \forall (f_1, f_2) \in \mathcal{F}_h^{b,opp}\}, \quad V_{\#}^h/\mathbb{R} = \{v_h \in V_{\#}^h \mid \int_{\Omega} v_h = 0\},$$

where $\mathcal{P}_1(K)$ denotes the space of all linear polynomials on K and $[\cdot]_f$ the jump across $(d-1)$ -dimensional face f . Let $\|\cdot\|_0$, $|\cdot|_1$, and $|\cdot|_{1,h}$ denote the standard L^2 -norm, H^1 -(semi-)norm, and mesh-dependent energy norm in Ω , respectively.

Here we define the concept of node-based functions. For a given node z in \mathcal{T}_h , let $\mathcal{F}_{(z)}$ denote the set of all $(d-1)$ -dimensional faces containing z . Then we can construct

a function $\phi_z \in V^h$ associated with z such that $\sigma_f^{(m)}(\phi_z) = \begin{cases} \frac{1}{2} & \text{if } f \in \mathcal{F}_{(z)}, \\ 0 & \text{otherwise,} \end{cases}$ where

m_f is the midpoint of $(d-1)$ -dimensional face f in \mathcal{F}_h . We call ϕ_z *the node-based function associated with z* . In the case of periodic BC for a rectangular domain Ω , we identify two boundary nodes in every opposite periodic position, and four nodes at the corners of the boundary. Using the node-based functions, we introduce a discrete function space and a set of functions, which will be used often:

$$V_{\#}^{\mathfrak{B},h} = \{v_h \in V_{\#}^h \mid v_h \in \text{Span } \mathfrak{B}\}, \quad (2.1a)$$

$$\mathfrak{B} = \{\phi_z\}_{z \in \mathcal{N}_h^{\#}} : \text{the set of all node-based functions in } V_{\#}^h, \quad (2.1b)$$

where $\mathcal{N}_h^\#$ denotes the set of all nodes with periodical identification. Notice that $|\mathfrak{B}| = N_x N_y$ in the 2D case, $|\mathfrak{B}| = N_x N_y N_z$ in the 3D case, due to identification between nodes on boundary. For $\mathfrak{S} \subset L^\infty(D)$, of size $|\mathfrak{S}|$ and a scalar-valued (integrable) function f , $\int_{\mathcal{D}} f \mathfrak{S}$ denotes a vector, of size $|\mathfrak{S}|$, such that each component is the integral of the product of f and the corresponding element in \mathfrak{S} over the domain \mathcal{D} . $\mathbf{1}_{\mathfrak{S}}$ denotes a vector, size of $|\mathfrak{S}|$, consisting of 1 for all components.

3. Dimension of the Finite Element Spaces.

3.1. Induced relation between boundary barycenter values. We consider a finite element space which approximates given function space with given BC. Then the barycenter values on boundary faces in the P_1 -nonconforming quadrilateral element space satisfy the following condition: for all $u \in V^h$

$$\sigma_{f_1}^{(m)}(u) + \sigma_{f_1^{\text{opp}}}^{(m)}(u) = \dots = \sigma_{f_d}^{(m)}(u) + \sigma_{f_d^{\text{opp}}}^{(m)}(u) \quad (3.1)$$

for all pairs $(f_j, f_j^{\text{opp}}) \in \mathcal{F}_h^{b, \text{opp}}(Q)$ for all $Q \in \mathcal{T}_h$, where $\mathcal{F}_h^{b, \text{opp}}(Q)$ denotes the set of all pairs consisting of two boundary faces on opposite position. We will coin the above formula (3.1) as *the dice rule*.

We will concentrate on the case of $d = 2$ in this section, and Sections 4–5. The 3 dimensional case will be covered in Section 6.

Let N_Q denote the number of all elements in \mathcal{T}_h . Let N_V , N_V^i , and N_V^b denote the number of all vertices, of all interior vertices, and of all boundary vertices, respectively. Similarly N_E , N_E^i , and N_E^b denote the number of all edges, of all interior edges, and of all boundary edges, respectively. The vertices in \mathcal{T}_h are grouped into Red and Black groups such that any two vertices connected by an edge in \mathcal{T}_h are not contained in the same group.

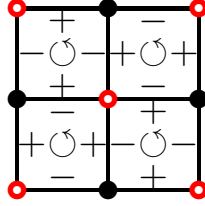


FIG. 3.1. For each element, the signs on its edges are chosen + if the edges are from a Black to Red vertices, and – otherwise.

A fixed orientation of edges is chosen throughout the all elements in \mathcal{T}_h . For instance, we impose the plus sign on an edge if its direction is from Red to Black, and the minus sign if the direction is opposite. The local signs on edges in each element induce a relation between 4 midpoint values on the element which corresponds to the dice rule:

$$\sum_{j=1}^4 (-1)^j \sigma_{f_j^K}^{(m)}(v_h) = 0, \quad \forall v_h \in V^h, f_j^K \text{ being the } j^{\text{th}} \text{ edge of } K, \forall K \in \mathcal{T}_h,$$

Since two local signs on both sides of an interior edge are always opposite, the sum of all locally induced relations reduces to a relation between midpoint values on boundary edges only. Note that the number of boundary edges in \mathcal{T}_h is always even and the remaining signs are alternating along the boundary. Figure 3.1 shows an example of orientation and induced signs on edges. The following lemma is easy but essential to the nonconforming P_1 element V^h .

LEMMA 3.1. *There exists a way to give alternating sign on boundary edges. Moreover, the alternating sum of boundary midpoint values of $v_h \in V^h$ is always zero, whenever the domain is simply connected.*

3.2. Minimally essential discrete BCs. Among all the midpoint values of a given essential BC only a subset of them is enough to impose consistent discrete boundary values. We call a set of discrete BCs *minimally essential* if essential boundary midpoint values in the set induce all other essential boundary midpoint values naturally, but any proper subset of the set does not.

Since each discrete essential BC removes the dimension of the space by 1, the number of subtracted DOFs due to essential BCs is just equal to the number of minimally essential discrete BCs. It recovers a well-known fact for the dimension of the finite element spaces with Neumann and homogeneous Dirichlet BC.

LEMMA 3.2. $\dim(V^h) = N_E - N_Q - \#(\text{minimally essential discrete BCs})$.

PROPOSITION 3.3. *For Neumann and Dirichlet BCs, we have*

$$\#(\text{minimally essential discrete BCs}) = \begin{cases} 0 & \text{for Neumann BC,} \\ N_E^b - 1 & \text{for homogeneous Dirichlet BC.} \end{cases}$$

Consequently, $\dim V^h = N_E - N_Q = N_V - 1$, and $\dim V_0^h = N_E - N_Q - (N_E^b - 1) = N_V^i$.

Remark 3.4. The proposition generalizes the dimensions for the homogeneous Dirichlet and Neumann BCs given in Theorems 2.5 and 2.8 in [27].

For periodic BCs, the conditions enforce two midpoint values on two opposite boundary edges to be equal. Therefore minimally essential discrete BCs form a smallest set of periodic relations between opposite boundary edges which induce all such periodic relations.

Depending on the parity of N_x and N_y , the behavior varies.

Case 1. First, suppose both N_x and N_y are even. We can easily derive the last periodic relation from the other periodic relations with the help of the relation between boundary midpoint values in Lemma 3.1. This means that a set of all periodic relations except any one of them is minimally essential.

Case 2. Next, consider the case where either N_x or N_y is odd. Then we can not have such a natural induction as in the Case 1, which means that a set of all periodic relations itself is minimally essential, see Figure 3.2.

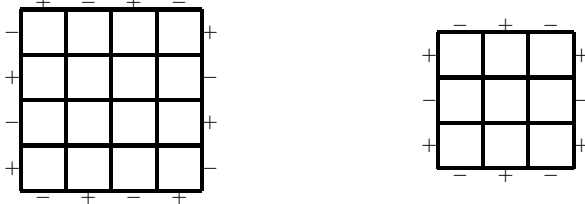


FIG. 3.2. *Induced relation between boundary midpoint values*

We summarize the above as in the following proposition:

PROPOSITION 3.5. *(Periodic BC) In the case of periodic BC on $N_x \times N_y$ rectangular mesh, $\#(\text{minimally essential discrete BCs}) = N_x + N_y - \mathbf{e}(N_x)\mathbf{e}(N_y)$. Consequently, $\dim V_{\#}^h = N_x N_y + \mathbf{e}(N_x)\mathbf{e}(N_y)$, where $\mathbf{e}(j) := \frac{1+(-1)^j}{2}$.*

4. Bases for Finite Element Spaces with Periodic BC. In this section, we investigate bases for $V_{\#}^h$.

4.1. Linear dependence of \mathfrak{B} . We write $\mathfrak{B} = \{\phi_{z_1}, \phi_{z_2}, \dots, \phi_{z_{|\mathfrak{B}|}}\}$, the set of all node-based functions in $V_{\#}^h$. Define a surjective linear map $B_h^{\mathfrak{B}} : \mathbb{R}^{|\mathfrak{B}|} \rightarrow V_{\#}^{\mathfrak{B},h}$ by $B_h^{\mathfrak{B}}(\mathbf{c}) = \sum_{j=1}^{|\mathfrak{B}|} c_j \phi_{z_j}$ where $\mathbf{c} = (c_j) \in \mathbb{R}^{|\mathfrak{B}|}$. For any $\mathbf{c} = (c_j) \in \ker B_h^{\mathfrak{B}}$, we have

$$c_k = -c_\ell \text{ for all vertex pair } (z_k, z_\ell) \text{ which are two end nodes of an edge.} \quad (4.1)$$

(4.1) means that $\dim \ker B_h^{\mathfrak{B}} \leq 1$. Due to the periodicity, those relations are consistent only if the number of discretization on each coordinate is even, and in such a case $\dim \ker B_h^{\mathfrak{B}} = 1$. Indeed, in this case any $|\mathfrak{B}| - 1$ functions in \mathfrak{B} form a basis for $V_{\#}^{\mathfrak{B},h}$. On the other hand, consider the case where either N_x or N_y is odd. Without loss of generality, we may assume that N_x is odd. Then a chain of such relation (4.1) along the x -direction cannot occur unless \mathbf{c} is trivial since the values at four values at the corners of Ω should match. This concludes that $\dim \ker B_h^{\mathfrak{B}} = 0$. We summarize the above result as the following proposition.

PROPOSITION 4.1. (*The dimension of $\ker B_h^{\mathfrak{B}}$ and $V_{\#}^{\mathfrak{B},h}$*)

$$\dim \ker B_h^{\mathfrak{B}} = \epsilon(N_x)\epsilon(N_y). \quad (4.2)$$

Moreover, $\mathfrak{B}^b = \{\phi_1, \dots, \phi_{|\mathfrak{B}|-1}\}$ forms a basis for $V_{\#}^{\mathfrak{B},h}$ if both N_x and N_y are even, whereas \mathfrak{B} itself is a basis for $V_{\#}^{\mathfrak{B},h}$ if either N_x or N_y is odd. Consequently,

$$\dim V_{\#}^{\mathfrak{B},h} = |\mathfrak{B}| - \dim \ker B_h^{\mathfrak{B}} = N_x N_y - \epsilon(N_x)\epsilon(N_y). \quad (4.3)$$

4.2. A basis for $V_{\#}^h$. First, consider the case where both N_x and N_y are even. Propositions 3.5 and 4.1 imply that \mathfrak{B} is linearly dependent and $V_{\#}^{\mathfrak{B},h}$ is a proper subset of $V_{\#}^h$ with $\dim(V_{\#}^h) - \dim(V_{\#}^{\mathfrak{B},h}) = 2\epsilon(N_x)\epsilon(N_y) = 2$, which means that there exist two *complementary basis functions* for $V_{\#}^h \setminus V_{\#}^{\mathfrak{B},h}$. Let us construct such basis functions. Define $\psi_x \in V_{\#}^h$ such that

$$\begin{aligned} & \text{its midpoint values on topologically vertical edges are } \pm 1 \\ & \text{with alternating sign in both directions and} \\ & \text{all the midpoint values on topologically horizontal edges are 0.} \end{aligned} \quad (4.4)$$

See Figure 4.1 (a) for an illustration for ψ_x . Notice that ψ_x is well-defined whenever N_x is even. It is easy to see that $\psi_x \notin V_{\#}^{\mathfrak{B},h}$. Similarly, we can find another piecewise linear function ψ_y in $V_{\#}^h$, not belonging to $V_{\#}^{\mathfrak{B},h}$ (Figure 4.1 (b)), such that its midpoint values on topologically horizontal edges are ± 1 with alternating sign in both directions and all the midpoint values on topologically vertical edges are 0. Next, let us consider the case where either N_x or N_y is odd. Propositions 3.5 and 4.1 imply that \mathfrak{B} is linearly independent and $\dim V_{\#}^{\mathfrak{B},h} = \dim V_{\#}^h$. Therefore $V_{\#}^{\mathfrak{B},h} = V_{\#}^h$ and \mathfrak{B} , the set of all node-based functions, is a basis for $V_{\#}^h$. We summarize these results as in following theorem.

THEOREM 4.2. (*A basis for $V_{\#}^h$*)

1. If both N_x and N_y are even, then $V_{\#}^{\mathfrak{B},h} \subsetneq V_{\#}^h$. Furthermore $\mathfrak{A} = \{\psi_x, \psi_y\}$ where ψ_x and ψ_y are defined as in (4.4), forms a complementary basis for

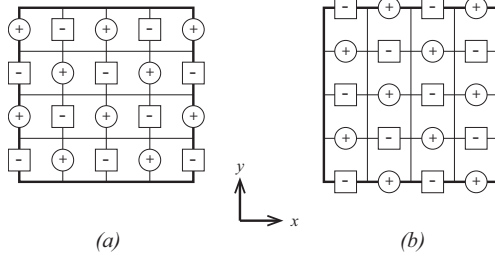


FIG. 4.1. An example of two alternating functions (a) ψ_x and (b) ψ_y . They do not belong to \mathfrak{B} .

$V_{\#}^h$, not belonging to $V_{\#}^{\mathfrak{B},h}$. Moreover, $\mathfrak{B}^b \cup \mathfrak{A}$ forms a basis for $V_{\#}^h$, where $\mathfrak{B}^b = \{\phi_1, \dots, \phi_{|\mathfrak{B}|-1}\}$.

2. If either N_x or N_y is odd, then $V_{\#}^{\mathfrak{B},h} = V_{\#}^h$. Moreover, \mathfrak{B} is a basis for $V_{\#}^h$.

Remark 4.3. Notice that the elementwise derivatives $\frac{\partial \psi_x}{\partial x}$ and $\frac{\partial \psi_y}{\partial y}$ are checkerboard patterns, while $\frac{\partial \psi_x}{\partial y} = \frac{\partial \psi_y}{\partial x} = 0$.

4.3. Stiffness matrix associated with \mathfrak{B} . Even though \mathfrak{B} may not be a basis for $V_{\#}^h$, it is still a useful set of functions to understand $V_{\#}^h$. Above all, the node-based functions are easy to handle in implementation viewpoint. Furthermore, Theorem 4.2 implies $V_{\#}^{\mathfrak{B},h}$, which equals to $\text{Span}(\mathfrak{B})$, occupies almost all of $V_{\#}^h$. In this section, we investigate some characteristics of \mathfrak{B} in approximating the Laplace operator.

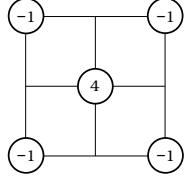


FIG. 4.2. The stencil for $\mathbf{S}_h^{\mathfrak{B}}$ with uniform cubes of size $h \times h$.

Set $\mathbf{S}_h^{\mathfrak{B}}$ be the $|\mathfrak{B}| \times |\mathfrak{B}|$ stiffness matrix associated with $\mathfrak{B} = \{\phi_j\}_{j=1}^{|\mathfrak{B}|}$, whose components are given by

$$(\mathbf{S}_h^{\mathfrak{B}})_{jk} = \sum_{K \in \mathcal{T}_h} \int_K \nabla \phi_k \cdot \nabla \phi_j \quad 1 \leq j, k \leq |\mathfrak{B}|. \quad (4.5)$$

The local stencil for the stiffness matrix associated with \mathfrak{B} is shown in Figure 4.2. Obviously, $\mathbf{S}_h^{\mathfrak{B}}$ is symmetric and positive semi-definite. The following lemma and proposition are immediate, but useful for later uses.

LEMMA 4.4. Let $v_h = \sum_j v_j \phi_j$ for $\mathbf{v} = (v_j) \in \mathbb{R}^{|\mathfrak{B}|}$. Then $\mathbf{v} \in \ker \mathbf{S}_h^{\mathfrak{B}}$ if and only if v_h is a constant function in Ω .

PROPOSITION 4.5. $\ker \mathbf{S}_h^{\mathfrak{B}}$ can be decomposed as

$$\ker \mathbf{S}_h^{\mathfrak{B}} = \ker B_h^{\mathfrak{B}} \oplus \text{Span } \mathbf{1}_{\mathfrak{B}}. \quad (4.6)$$

Remark 4.6. Lemma 4.4 and Proposition 4.5 are also valid in the 3D case.

Observe that Propositions 4.1 and 4.5 directly lead to the following proposition.

PROPOSITION 4.7. (The dimension of $\ker \mathbf{S}_h^{\mathfrak{B}}$)

$$\dim \ker \mathbf{S}_h^{\mathfrak{B}} = \mathfrak{c}(N_x)\mathfrak{c}(N_y) + 1. \quad (4.7)$$

5. Numerical Schemes for Elliptic Problems with Periodic BC. Assume that $f \in L^2(\Omega)$ is given such that $\int_{\Omega} f = 0$. Consider the elliptic problem with periodic BC to find $u \in H_{\#}^1(\Omega)/\mathbb{R}$ such that $-\Delta u = f$ in Ω . The weak formulation is as follows: find $u \in H_{\#}^1(\Omega)/\mathbb{R}$ such that

$$\int_{\Omega} \nabla u \cdot \nabla v = \int_{\Omega} f v \quad \forall v \in H_{\#}^1(\Omega)/\mathbb{R}. \quad (5.1)$$

By defining $a_h(u_h, v_h) := \sum_{K \in \mathcal{T}_h} \int_K \nabla u_h \cdot \nabla v_h$, the discrete weak formulation for (5.1) is given as follows: find $u_h \in V_{\#}^h/\mathbb{R}$ such that

$$a_h(u_h, v_h) = \int_{\Omega} f v_h \quad \forall v_h \in V_{\#}^h/\mathbb{R}. \quad (5.2)$$

Remark 5.1. Throughout this section, we assume that both N_x and N_y are even. The other cases with odd N_x and/or N_y are easy to handle owing to $V_{\#}^h = V_{\#}^{\mathfrak{B},h}$. Also we will assume that $(\mathcal{T}_h)_{0 < h}$ is a family of uniform rectangular decomposition.

Additional Notations & Properties. We compare 4 different numerical approaches to solve (5.2) with the trial and test function spaces $\mathcal{S} = \mathfrak{B}^b, \mathfrak{B}, \mathfrak{E}^b, \mathfrak{E}$, which are described as follows. Due to Proposition 4.1, we can find \mathfrak{B}^b , a proper subset of \mathfrak{B} , which is a basis for $V_{\#}^{\mathfrak{B},h}$. It clearly holds that $|\mathfrak{B}^b| = \dim V_{\#}^{\mathfrak{B},h} = |\mathfrak{B}| - 1$. Consider the two extended sets $\mathfrak{E} := \mathfrak{B} \cup \mathfrak{A}$ and $\mathfrak{E}^b := \mathfrak{B}^b \cup \mathfrak{A}$, the latter of which is a basis for $V_{\#}^h$. The characteristics of $\mathfrak{B}^b, \mathfrak{B}, \mathfrak{E}^b$, and \mathfrak{E} are summarized in Table 5.1. For a vector \mathbf{v} with $|\mathfrak{E}|$ (or $|\mathfrak{E}^b|$) number of components, let $\mathbf{v}|_{\mathfrak{B}}$ (or $\mathbf{v}|_{\mathfrak{B}^b}$)

\mathcal{S}	$ \mathcal{S} $	$\text{Span } \mathcal{S}$	$\dim \text{Span } \mathcal{S}$
\mathfrak{B}^b	$N_x N_y - 1$	$V_{\#}^{\mathfrak{B},h}$	$N_x N_y - 1$
\mathfrak{B}	$N_x N_y$		
\mathfrak{E}^b	$N_x N_y + 1$	$V_{\#}^h$	$N_x N_y + 1$
\mathfrak{E}	$N_x N_y + 2$		

TABLE 5.1

Characteristics of each test and trial function set \mathcal{S} when both N_x, N_y are even

and $\mathbf{v}|_{\mathfrak{A}}$ denote vectors consisting of the first $|\mathfrak{B}|$ (or $|\mathfrak{B}^b|$) components, and of the last $|\mathfrak{A}|$ components, respectively. Several properties of functions in \mathfrak{B} and \mathfrak{A} can be observed.

LEMMA 5.2. Let \mathfrak{B} and \mathfrak{A} be as above. Then the followings hold.

1. $a_h(\phi, \psi) = 0 \forall \phi \in \mathfrak{B} \forall \psi \in \mathfrak{A}$.
2. $a_h(\psi_{\mu}, \psi_{\nu}) = 0 \forall \psi_{\mu}, \psi_{\nu} \in \mathfrak{A}$ such that $\mu \neq \nu$.
3. $\int_{\Omega} \psi = 0 \forall \psi \in \mathfrak{A}$.
4. There exists an h -independent constant C such that $\|\psi\|_0 \leq C$ and $|\psi|_{1,h} \leq Ch^{-1} \forall \psi \in \mathfrak{A}$.

Now, we define a stiffness matrix associated with \mathfrak{B}^b , and its variants. Let $\mathbf{S}_h^{\mathfrak{B}^b}$ be the $|\mathfrak{B}^b| \times |\mathfrak{B}^b|$ stiffness matrix associated with \mathfrak{B}^b whose components are given by

$$(\mathbf{S}_h^{\mathfrak{B}^b})_{jk} := a_h(\phi_k, \phi_j) \quad 1 \leq j, k \leq |\mathfrak{B}^b|, \quad (5.3)$$

and $\tilde{\mathbf{S}}_h^{\mathfrak{B}^b}$ be the same matrix as $\mathbf{S}_h^{\mathfrak{B}^b}$, but the last row is modified in order to impose the zero mean value condition. Because all the integrals $\int_{\Omega} \phi_j$ are same for all ϕ_j in \mathfrak{B} , every entry in the last row is replaced by 1.

$$(\tilde{\mathbf{S}}_h^{\mathfrak{B}^b})_{jk} := \begin{cases} a_h(\phi_k, \phi_j) & j \neq |\mathfrak{B}^b|, \\ 1 & j = |\mathfrak{B}^b|. \end{cases} \quad (5.4)$$

Note that $\tilde{\mathbf{S}}_h^{\mathfrak{B}^b}$ is nonsingular whereas both $\mathbf{S}_h^{\mathfrak{B}}$ and $\mathbf{S}_h^{\mathfrak{B}^b}$ are singular with rank deficiency 2 and 1, respectively. For the complementary part, let $\mathbf{S}_h^{\mathfrak{A}}$ be the $|\mathfrak{A}| \times |\mathfrak{A}|$ stiffness matrix associated with \mathfrak{A} ,

$$(\mathbf{S}_h^{\mathfrak{A}})_{jk} := a_h(\psi_k, \psi_j) \quad 1 \leq j, k \leq |\mathfrak{A}|. \quad (5.5)$$

Notice that $\mathbf{S}_h^{\mathfrak{A}}$ is a nonsingular diagonal matrix due to Lemma 5.2.

5.1. Option 1: $\mathcal{S} = \mathfrak{E}^b$ for a nonsingular nonsymmetric system. Since \mathfrak{E}^b is a basis for $V_{\#}^h$, \mathfrak{E}^b is a natural choice as a set of trial and test functions to assemble a linear system corresponding to (5.2). The numerical solution $u_h \in V_{\#}^h$ is uniquely expressed, associated with \mathfrak{E}^b , as

$$u_h = \tilde{\mathbf{u}}^b \mathfrak{E}^b \quad (5.6)$$

where $\tilde{\mathbf{u}}^b$ is the solution of the following system of equations associated with \mathfrak{E}^b :

$$\tilde{\mathcal{L}}_h^{\mathfrak{E}^b} \tilde{\mathbf{u}}^b = \begin{bmatrix} \tilde{\mathbf{f}}_{\mathfrak{B}^b} \\ \mathbf{f}_{\mathfrak{A}} \end{bmatrix} \quad (5.7)$$

where $\tilde{\mathcal{L}}_h^{\mathfrak{E}^b} := \begin{bmatrix} \tilde{\mathbf{S}}_h^{\mathfrak{B}^b} & \mathbf{0} \\ \mathbf{0} & \mathbf{S}_h^{\mathfrak{A}} \end{bmatrix}$, $(\tilde{\mathbf{f}}_{\mathfrak{B}^b})_j = \begin{cases} \int_{\Omega} f \phi_j, & 1 \leq j < |\mathfrak{B}^b| \\ 0, & j = |\mathfrak{B}^b| \end{cases}$, and $\mathbf{f}_{\mathfrak{A}} = \int_{\Omega} f \mathfrak{A}$. Due to Lemma 5.2, $\tilde{\mathcal{L}}_h^{\mathfrak{E}^b}$ is a block-diagonal matrix. Moreover, it is nonsingular, but nonsymmetric due to the modification in the last row of $\tilde{\mathbf{S}}_h^{\mathfrak{B}^b}$ which comes from the zero mean value condition. We can use any known numerical scheme for general linear systems, for instance GMRES, to solve (5.7).

SCHEME 1. GMRES for $\mathcal{S} = \mathfrak{E}^b$

Step 1. Take an initial vector $\mathbf{u}^{(0)} \in \mathbb{R}^{|\mathfrak{E}^b|}$.

Step 2. Solve the nonsymmetric system (5.7) by a restarted GMRES and set $\tilde{\mathbf{u}}^b := \mathbf{u}^{(n)}$.

Step 3. The numerical solution is obtained as $u_h = \tilde{\mathbf{u}}^b \mathfrak{E}^b$.

5.2. Option 2: $\mathcal{S} = \mathfrak{E}^b$ for a symmetric positive semi-definite system with rank deficiency 1. In the previous approach, the zero mean value condition is imposed in a system of equations directly. Consequently the associated linear system becomes nonsymmetric due to modification of just a single row.

In this subsection we will impose the zero mean value condition indirectly in order to conserve symmetry of the assembled linear system. In particular, we will impose the zero mean value condition in post-processing stage. Then we can apply some fast solvers for symmetric system. On the other hand, nonsingularity can not be avoided any longer in this approach. Fortunately the linear system is at least positive semi-definite. Hence we can use a Drazin inverse as mentioned in Section 2.1 to solve our singular system using a Krylov iterative method under a proper condition.

Consider a system of equations for (5.2) associated with \mathfrak{E}^b without any modification:

$$\mathcal{L}_h^{\mathfrak{E}^b} \mathbf{u}^b = \int_{\Omega} f \mathfrak{E}^b \quad \text{where} \quad \mathcal{L}_h^{\mathfrak{E}^b} := \begin{bmatrix} \mathbf{S}_h^{\mathfrak{B}^b} & \mathbf{0} \\ \mathbf{0} & \mathbf{S}_h^{\mathfrak{A}} \end{bmatrix}. \quad (5.8)$$

Note that the above linear system is singular, and symmetric positive semi-definite. We should find the solution \mathbf{u}^b of the system such that

$$\mathbf{u}^b|_{\mathfrak{B}^b} \cdot \mathbf{1}_{\mathfrak{B}^b} = 0 \quad (5.9)$$

since $\int_{\Omega} \mathbf{v} \mathfrak{E}^b = 0$ if and only if $\mathbf{v}|_{\mathfrak{B}^b} \cdot \mathbf{1}_{\mathfrak{B}^b} = 0$, and the numerical solution $u_h^b \in V_{\#}^b$ of this scheme is obtained by

$$u_h^b = \mathbf{u}^b \mathfrak{E}^b. \quad (5.10)$$

If a symmetric positive semi-definite system $Ax = b$ is given, as our formulation above, the conjugate gradient method (CG) gives a unique Krylov solution if the consistency condition $b \in \text{Im } A$ holds. The general solution is obviously obtained upto its kernel. The kernel of the linear system (5.8) is closely related with the kernel of $\mathbf{S}_h^{\mathfrak{B}^b}$. A simple analog of Section 4.3 implies that the dimension of $\ker \mathbf{S}_h^{\mathfrak{B}^b}$ is 1, and $\mathbf{v} \in \ker \mathbf{S}_h^{\mathfrak{B}^b}$ if and only if $\mathbf{v} \mathfrak{B}^b$ is a constant function in Ω . Note that \mathfrak{B}^b is not a partition of unity, whereas \mathfrak{B} is. Let $\mathbf{w}_{\mathfrak{B}^b}$ denote a unique vector in $\mathbb{R}^{|\mathfrak{B}^b|}$ such that $\mathbf{w}_{\mathfrak{B}^b} \mathfrak{B}^b \equiv 1$ in Ω . Then the kernel of the linear system in (5.8) is simply represented by $\text{Span } \mathbf{w}_{\mathfrak{E}^b}$ where

$$\mathbf{w}_{\mathfrak{E}^b} = [\mathbf{w}_{\mathfrak{B}^b}^T \quad \mathbf{0}]^T \in \mathbb{R}^{|\mathfrak{E}^b|}$$

is the trivial extension of $\mathbf{w}_{\mathfrak{B}^b}$. Therefore in the post-processing stage we add a multiple of $\mathbf{w}_{\mathfrak{E}^b}$ to the Krylov solution to preserve (5.9).

In summary, the numerical scheme for u_h^b is given as follows.

SCHEME 2. CG for $\mathcal{S} = \mathfrak{E}^b$ of rank 1 deficiency

Step 1. Take a vector $\mathbf{u}^{(0)} \in \mathbb{R}^{|\mathfrak{E}^b|}$ for an initial guess.

Step 2. Solve the singular symmetric positive semi-definite system (5.8) by the CG and get the Krylov solution $\mathbf{u}' = \mathbf{u}^{(n)}$.

Step 3. Add a multiple of $\mathbf{w}_{\mathfrak{E}^b}$ to \mathbf{u}' to get \mathbf{u}^b , in order to enforce (5.9), as

$$\mathbf{u}^b = \mathbf{u}' - \frac{\mathbf{u}'|_{\mathfrak{B}^b} \cdot \mathbf{1}_{\mathfrak{B}^b}}{\mathbf{w}_{\mathfrak{B}^b} \cdot \mathbf{1}_{\mathfrak{B}^b}} \mathbf{w}_{\mathfrak{E}^b}.$$

Step 4. The numerical solution is obtained as $u_h^b = \mathbf{u}^b \mathfrak{E}^b$.

5.3. Option 3: $\mathcal{S} = \mathfrak{E}$ for a symmetric positive semi-definite system with rank deficiency 2. Although symmetry and positive semi-definiteness are key factors for an efficient numerical scheme for linear solvers, we may not enjoy full benefits in the previous scheme. We need the extra post-processing stage to impose the zero mean value condition. The defect in the previous approach comes from the fact that the Riesz representation vector for the integral functional does not belong to the kernel of the linear system. As shown above, the kernel of the linear system is closely related with the coefficient vector for the unity function. If these two vectors coincide, we can get our solution without any post-processing stage. The imbalance of \mathfrak{B}^b for the linear independence is also a disadvantage to numerical implementation.

In this approach, we find the numerical solution $u_h^{\natural} \in V_{\#}^h$ such that

$$u_h^{\natural} = \mathbf{u}^{\natural} \mathfrak{E} \quad (5.11)$$

where \mathbf{u}^{\natural} is a solution of a system of equations for (5.2) associated with full \mathfrak{E} ,

$$\mathcal{L}_h^{\mathfrak{E}} \mathbf{u}^{\natural} := \begin{bmatrix} \mathbf{S}_h^{\mathfrak{B}} & \mathbf{0} \\ \mathbf{0} & \mathbf{S}_h^{\mathfrak{A}} \end{bmatrix} \mathbf{u}^{\natural} = \int_{\Omega} f \mathfrak{E} \quad (5.12)$$

with

$$\mathbf{u}^{\natural}|_{\mathfrak{B}} \cdot \mathbf{1}_{\mathfrak{B}} = 0, \quad (5.13)$$

since $\int_{\Omega} \mathbf{v} \mathfrak{E} = 0$ if and only if $\mathbf{v}|_{\mathfrak{B}} \cdot \mathbf{1}_{\mathfrak{B}} = 0$. The numerical solution u^{\natural} is unique because a solution of the linear system is unique upto an additive nontrivial representation for the zero function in \mathfrak{B} . We want to emphasize that, unlike the previous scheme, $\mathbf{1}_{\mathfrak{B}}$ belongs to the kernel of $\mathbf{S}_h^{\mathfrak{B}}$ as shown in (4.5). It implies that, without any extra post-processing stage, we can find the solution of the linear system which satisfies the zero mean value condition (5.13) if an initial guess is chosen to satisfy the same condition.

In summary, we have the numerical solution u_h^{\natural} as follows.

SCHEME 3. CG for $\mathcal{S} = \mathfrak{E}$ of rank 2 deficiency

Step 1. Take an initial vector $\mathbf{u}^{(0)} \in \mathbb{R}^{|\mathfrak{E}|}$ which satisfies $\mathbf{u}^{(0)}|_{\mathfrak{B}} \cdot \mathbf{1}_{\mathfrak{B}} = 0$.

Step 2. Solve the singular symmetric positive semi-definite system (5.12) by the CG and get the Krylov solution $\mathbf{u}^{\natural} = \mathbf{u}^{(n)}$.

Step 3. The numerical solution is obtained as $u_h^{\natural} = \mathbf{u}^{\natural} \mathfrak{E}$.

5.4. Option 4: $\mathcal{S} = \mathfrak{B}$ for a symmetric positive semi-definite system with rank deficiency 2. Consider a system of equations associated only with \mathfrak{B} for (5.2) to find $\bar{u}_h^{\natural} \in V_{\#}^{\mathfrak{B},h}$ such that

$$\mathcal{L}_h^{\mathfrak{B}} \bar{\mathbf{u}}^{\natural} := \mathbf{S}_h^{\mathfrak{B}} \bar{\mathbf{u}}^{\natural} = \int_{\Omega} f \mathfrak{B}. \quad (5.14)$$

Starting from an initial vector $\mathbf{u}^{(0)} \in \mathbb{R}^{|\mathfrak{B}|}$ which satisfies $\mathbf{u}^{(0)} \cdot \mathbf{1}_{\mathfrak{B}} = 0$, let $\bar{\mathbf{u}}^{\natural}$ be the Krylov solution of the linear system. The numerical solution $\bar{u}_h^{\natural} \in V_{\#}^{\mathfrak{B},h}$ is obtained by

$$\bar{u}_h^{\natural} = \bar{\mathbf{u}}^{\natural} \mathfrak{B}. \quad (5.15)$$

We summarize the above procedure as follows.

SCHEME 4. CG for $\mathcal{S} = \mathfrak{B}$ of rank 2 deficiency

Step 1. Take an initial vector $\mathbf{u}^{(0)} \in \mathbb{R}^{|\mathfrak{E}|}$ which satisfies $\mathbf{u}^{(0)}|_{\mathfrak{B}} \cdot \mathbf{1}_{\mathfrak{B}} = 0$.

Step 2. Solve the singular symmetric positive semi-definite system (5.14) by the CG and get the Krylov solution $\bar{\mathbf{u}}^{\natural} = \mathbf{u}^{(n)}$.

Step 3. The numerical solution is obtained as $\bar{u}_h^{\natural} = \bar{\mathbf{u}}^{\natural} \mathfrak{B}$.

Main Theorem: Relation Between Numerical Solutions. The following theorem states the relation between all numerical solutions discussed above.

THEOREM 5.3. Let $(\mathcal{T}_h)_{0 < h}$ be a family of uniform rectangular decomposition, that is, $\mathcal{T}_h = \tilde{\mathcal{T}}_h$ for all h . Assume that N_x and N_y are even. Let $u_h, u_h^{\flat}, u_h^{\natural}, \bar{u}_h^{\natural}$ be

the numerical solutions of (5.1) as (5.6), (5.10), (5.11), (5.15), respectively. Then $u_h = u_h^b = u_h^{\natural}$, and

$$\|u_h^{\natural} - \bar{u}_h^{\natural}\|_0 \leq Ch^2 \|f\|_0, \quad |u_h^{\natural} - \bar{u}_h^{\natural}|_{1,h} \leq Ch \|f\|_0.$$

Remark 5.4. Theorem 5.3 provides theoretical error bounds with a set of test and trial functions which are redundant but easy to implement, instead of a set of exact solutions which are exactly fitted but complicated to implement.

Proof. Let \mathbf{u}^b and $\bar{\mathbf{u}}^b$ be the solutions as in Sections 5.1 and 5.2, respectively. Note that two linear systems (5.7) and (5.8) coincide except $|\mathfrak{B}^b|$ -th row. Even on $|\mathfrak{B}^b|$ -th row,

$$\begin{aligned} \left(\tilde{\mathcal{L}}_h^{\mathfrak{E}^b} \mathbf{u}^b\right)_{|\mathfrak{B}^b|} &= \mathbf{1}_{\mathfrak{B}^b} \cdot \left(\mathbf{u}' - \frac{\mathbf{u}'|_{\mathfrak{B}^b} \cdot \mathbf{1}_{\mathfrak{B}^b}}{\mathbf{w}_{\mathfrak{B}^b} \cdot \mathbf{1}_{\mathfrak{B}^b}} \mathbf{w}_{\mathfrak{E}^b}\right)_{|\mathfrak{B}^b|} \\ &= \mathbf{1}_{\mathfrak{B}^b} \cdot \left(\mathbf{u}'|_{\mathfrak{B}^b} - \frac{\mathbf{u}'|_{\mathfrak{B}^b} \cdot \mathbf{1}_{\mathfrak{B}^b}}{\mathbf{w}_{\mathfrak{B}^b} \cdot \mathbf{1}_{\mathfrak{B}^b}} \mathbf{w}_{\mathfrak{B}^b}\right) \\ &= 0. \end{aligned}$$

Thus $\tilde{\mathcal{L}}_h^{\mathfrak{E}^b} \mathbf{u}^b = \begin{bmatrix} \tilde{\mathbf{f}}_{\mathfrak{B}^b} \\ \tilde{\mathbf{f}}_{\mathfrak{A}} \end{bmatrix} = \tilde{\mathcal{L}}_h^{\mathfrak{E}^b} \bar{\mathbf{u}}^b$, and it implies $\mathbf{u}^b = \bar{\mathbf{u}}^b$ because $\tilde{\mathcal{L}}_h^{\mathfrak{E}^b}$ is nonsingular. It concludes $u_h = u_h^b$.

Let \mathbf{u}^{\natural} be the solution as in Section 5.3. Then, we have $\mathbf{u}^{\natural}|_{\mathfrak{A}} = \mathbf{u}^b|_{\mathfrak{A}}$. Let $\begin{bmatrix} \mathbf{u}^b|_{\mathfrak{B}^b} \\ 0 \end{bmatrix}$ be a trivial extension of $\mathbf{u}^b|_{\mathfrak{B}^b}$ into a vector in $\mathbb{R}^{|\mathfrak{B}|}$ by padding a single zero. Note that $\sum_{j=1}^{|\mathfrak{B}|} (\mathbf{S}_h^{\mathfrak{B}})_{jk} = 0$ for all $1 \leq k \leq |\mathfrak{B}|$. Due to the definition of \mathbf{u}^b , we have

$$\begin{aligned} \mathbf{S}_h^{\mathfrak{B}} \begin{bmatrix} \mathbf{u}^b|_{\mathfrak{B}^b} \\ 0 \end{bmatrix} &= \begin{bmatrix} \mathbf{S}_h^{\mathfrak{B}^b} \mathbf{u}^b|_{\mathfrak{B}^b} \\ [\mathbf{S}_h^{\mathfrak{B}}]_{|\mathfrak{B}|,1:|\mathfrak{B}^b|} \mathbf{u}^b|_{\mathfrak{B}^b} \end{bmatrix} = \begin{bmatrix} \int_{\Omega} f \mathfrak{B}^b \\ - \sum_{j \neq |\mathfrak{B}|} [\mathbf{S}_h^{\mathfrak{B}}]_{j,1:|\mathfrak{B}^b|} \mathbf{u}^b|_{\mathfrak{B}^b} \end{bmatrix} \\ &= \begin{bmatrix} \int_{\Omega} f \mathfrak{B}^b \\ - \sum_{j=1}^{|\mathfrak{B}^b|} [\mathbf{S}_h^{\mathfrak{B}^b}]_{j,1:|\mathfrak{B}^b|} \mathbf{u}^b|_{\mathfrak{B}^b} \end{bmatrix} = \begin{bmatrix} \int_{\Omega} f \mathfrak{B}^b \\ - \sum_{j=1}^{|\mathfrak{B}^b|} \int_{\Omega} f \phi_j \end{bmatrix} \\ &= \begin{bmatrix} \int_{\Omega} f \mathfrak{B}^b \\ \int_{\Omega} f (\phi_{|\mathfrak{B}|} - 1) \end{bmatrix} = \int_{\Omega} f \mathfrak{B}, \end{aligned}$$

since \mathfrak{B} is a partition of unity and $\int_{\Omega} f = 0$. On the other hand, the definition of \mathbf{u}^{\natural} implies $\mathbf{S}_h^{\mathfrak{B}} \mathbf{u}^{\natural}|_{\mathfrak{B}} = \int_{\Omega} f \mathfrak{B}$. Thus $\mathbf{u}^{\natural}|_{\mathfrak{B}} - \begin{bmatrix} \mathbf{u}^b|_{\mathfrak{B}^b} \\ 0 \end{bmatrix}$ is in the kernel of $\mathbf{S}_h^{\mathfrak{B}}$, which is decomposed as Proposition 4.5. Due to the zero mean value condition in each scheme, $\left(\mathbf{u}^{\natural}|_{\mathfrak{B}} - \begin{bmatrix} \mathbf{u}^b|_{\mathfrak{B}^b} \\ 0 \end{bmatrix}\right) \cdot \mathbf{1}_{\mathfrak{B}} = \mathbf{u}^{\natural}|_{\mathfrak{B}} \cdot \mathbf{1}_{\mathfrak{B}} - \mathbf{u}^b|_{\mathfrak{B}^b} \cdot \mathbf{1}_{\mathfrak{B}^b} = 0$. Therefore $\mathbf{u}^{\natural}|_{\mathfrak{B}} - \begin{bmatrix} \mathbf{u}^b|_{\mathfrak{B}^b} \\ 0 \end{bmatrix}$ must belong to $\ker B_h^{\mathfrak{B}}$, and consequently $\left(\mathbf{u}^{\natural}|_{\mathfrak{B}} - \begin{bmatrix} \mathbf{u}^b|_{\mathfrak{B}^b} \\ 0 \end{bmatrix}\right) \mathfrak{B} = \mathbf{u}^{\natural}|_{\mathfrak{B}} \mathfrak{B} - \mathbf{u}^b|_{\mathfrak{B}^b} \mathfrak{B}^b$ is equal to 0. This implies $u_h^{\natural} = u_h^b$.

Let $\bar{\mathbf{u}}^{\natural}$ be the solution as in Section 5.4. Note that $\mathbf{u}^{\natural}|_{\mathfrak{B}} = \bar{\mathbf{u}}^{\natural}$, and

$$\mathbf{u}^{\natural}|_{\mathfrak{A}} = \text{diag}(a_h(\psi_x, \psi_x), a_h(\psi_y, \psi_y))^{-1} \int_{\Omega} f \mathfrak{A} \leq Ch^2 \int_{\Omega} f \mathfrak{A}$$

h	Opt 1				Opt 2			
	$ u - u_h _{1,h}$	order	$\ u - u_h\ _0$	order	$ u - u_h^b _{1,h}$	order	$\ u - u_h^b\ _0$	order
1/8	1.123E+01	-	4.230E-01	-	1.123E+01	-	4.230E-01	-
1/16	5.466E-00	1.039	8.607E-02	2.297	5.466E-00	1.039	8.607E-02	2.297
1/32	2.832E-00	0.949	2.216E-02	1.957	2.832E-00	0.949	2.216E-02	1.957
1/64	1.429E-00	0.987	5.585E-03	1.989	1.429E-00	0.987	5.585E-03	1.989
1/128	7.160E-01	0.997	1.399E-03	1.997	7.160E-01	0.997	1.399E-03	1.997
1/256	3.582E-01	0.999	3.499E-04	1.999	3.582E-01	0.999	3.499E-04	1.999

h	Opt 3				Opt 4			
	$ u - u_h^{\sharp} _{1,h}$	order	$\ u - u_h^{\sharp}\ _0$	order	$ u - \bar{u}_h^{\sharp} _{1,h}$	order	$\ u - \bar{u}_h^{\sharp}\ _0$	order
1/8	1.123E+01	-	4.230E-01	-	1.123E+01	-	4.230E-01	-
1/16	5.466E-00	1.039	8.607E-02	2.297	5.466E-00	1.039	8.607E-02	2.297
1/32	2.832E-00	0.949	2.216E-02	1.957	2.832E-00	0.949	2.216E-02	1.957
1/64	1.429E-00	0.987	5.585E-03	1.989	1.429E-00	0.987	5.585E-03	1.989
1/128	7.160E-01	0.997	1.399E-03	1.997	7.160E-01	0.997	1.399E-03	1.997
1/256	3.582E-01	0.999	3.499E-04	1.999	3.582E-01	0.999	3.499E-04	1.999

TABLE 5.2
Numerical results for Example 5.5.

due to Lemma 5.2. Owing to $\int_{\Omega} f\psi \leq C (\int_{\Omega} |f|^2)^{1/2} (\int_{\Omega} |\psi|^2)^{1/2} \leq C \|f\|_0 \forall \psi \in \mathfrak{A}$, each component of $\mathbf{u}^{\sharp}|_{\mathfrak{A}}$ is bounded by $\mathcal{O}(h^2)$. Hence we have desired estimates the difference between u_h^{\sharp} and \bar{u}_h^{\sharp} in L^2 - and H^1 -(semi-)norm. \square

5.5. Numerical results. For the scheme Option 1, we use the restarted GMRES scheme in MGMRES library provided by Ju and Burkardt [21]. We emphasize that we replace one of essentially linearly dependent rows of $\mathbf{S}_h^{\mathfrak{B}^b}$ by the zero mean value condition in order to make $\tilde{\mathbf{S}}_h^{\mathfrak{B}^b}$ nonsingular.

EXAMPLE 5.5. Consider the problem (5.1) on the domain $\Omega = (0, 1)^2$ with the exact solution $u(x, y) = s(x)s(y)$ where $s(t) = \sum_{k=1}^3 \frac{4}{(2k-1)\pi} \sin(2(2k-1)\pi t)$, a truncated Fourier series for the square wave.

For each option, the error in energy norm and L^2 -norm for Example 5.5 are shown in Table 5.2. We observe that all schemes give very similar numerical solutions.

EXAMPLE 5.6. Consider the same problem as in Example 5.5 with the exact solution $u(x, y) = s(x)s(y)$ where $s(t) = \exp\left(-\frac{1}{1-(2t-1)^2}\right) t^2(1-t) + C$, with a constant C satisfying $\int_{[0,1]} s = 0$.

Table 5.3 shows numerical results for Example 5.6 in each option, and all options give almost the same result, as the previous example. The iteration number and elapsed time in each option in the case of $h = 1/256$ are shown in Table 5.4. We observe decrease of the iteration number and elapsed time in the option 3 compared to the option 2. Decrease from the option 3 to the option 4 is quite natural because we only use the node-based functions as trial and test functions for the option 4.

6. Extension to the 3D Case. In this section we consider the case of $d = 3$.

6.1. Dimension of finite element spaces in 3D. The following lemma is the 3D analog of Lemma 3.2.

LEMMA 6.1. For $\Omega \subset \mathbb{R}^3$, we have

$$\dim(V^h) = \#(\text{faces}) - 2\#(\text{cells}) - \#(\text{minimally essential discrete BCs}).$$

h	Opt 1				Opt 2			
	$ u - u_h _{1,h}$	order	$\ u - u_h\ _0$	order	$ u - u_h^b _{1,h}$	order	$\ u - u_h^b\ _0$	order
1/8	1.225E-03	-	5.649E-05	-	1.225E-03	-	5.649E-05	-
1/16	6.024E-04	1.024	1.033E-05	2.450	6.024E-04	1.024	1.033E-05	2.450
1/32	3.045E-04	0.984	1.949E-06	2.406	3.045E-04	0.984	1.949E-06	2.406
1/64	1.527E-04	0.996	4.682E-07	2.058	1.527E-04	0.996	4.682E-07	2.058
1/128	7.642E-05	0.999	1.171E-07	1.999	7.642E-05	0.999	1.171E-07	1.999
1/256	3.822E-05	1.000	2.929E-08	2.000	3.822E-05	1.000	2.929E-08	2.000

h	Opt 3				Opt 4			
	$ u - u_h^{\sharp} _{1,h}$	order	$\ u - u_h^{\sharp}\ _0$	order	$ u - \bar{u}_h^{\sharp} _{1,h}$	order	$\ u - \bar{u}_h^{\sharp}\ _0$	order
1/8	1.225E-03	-	5.649E-05	-	1.225E-03	-	5.649E-05	-
1/16	6.024E-04	1.024	1.033E-05	2.450	6.024E-04	1.024	1.033E-05	2.450
1/32	3.045E-04	0.984	1.949E-06	2.406	3.045E-04	0.984	1.949E-06	2.406
1/64	1.527E-04	0.996	4.682E-07	2.058	1.527E-04	0.996	4.682E-07	2.058
1/128	7.642E-05	0.999	1.171E-07	1.999	7.642E-05	0.999	1.171E-07	1.999
1/256	3.822E-05	1.000	2.929E-08	2.000	3.822E-05	1.000	2.929E-08	2.000

TABLE 5.3
Numerical results for Example 5.6.

	solver	iter	time (sec.)
Opt 1	GMRES(20)	4944	61.52
Opt 2	CG	817	3.30
Opt 3	CG	437	1.80
Opt 4	CG	318	1.33

TABLE 5.4
Iteration number and elapsed time in each option with 256×256 mesh

Proof. We can rewrite the dice rule in a single 3D cubic cell $K \in \mathcal{T}_h$ into two separated relations:

$$\begin{aligned} v_h(m_1^K) - v_h(m_2^K) + v_h(m_6^K) - v_h(m_5^K) &= 0, \\ v_h(m_1^K) - v_h(m_3^K) + v_h(m_6^K) - v_h(m_4^K) &= 0 \end{aligned}$$

for all $v_h \in V^h$ where m_j^K is the barycenter of face f_j^K of K , and the faces are arranged to satisfy that the sum of indices in opposite faces is equal to 7, as an ordinary dice. Since each relation reduces the number of DOFs in the finite element space by 1, same as in the 2D case, the claim is derived in consequence. \square

PROPOSITION 6.2. (Neumann and Dirichlet BCs in 3D)

$$\begin{aligned} &\#(\text{minimally essential discrete BCs}) \\ &= \begin{cases} 0 & \text{for Neumann BC,} \\ 2(N_x N_y + N_y N_z + N_z N_x) & \text{with homogeneous Dirichlet BC} \\ \quad - (N_x + N_y + N_z) + 1 & \end{cases} \end{aligned}$$

Consequently,

$$\dim V^h = N_V - 1, \quad (6.1a)$$

$$\dim V_0^h = N_V^i. \quad (6.1b)$$

Proof. It is enough to consider the homogeneous Dirichlet boundary case since there is nothing to prove in the Neumann case. Suppose that the homogeneous Dirichlet BC is given. Similarly to the argument in 2D, we need to investigate induced relations on boundary barycenter values. Consider the topological x -direction first, and classify all cells into N_x groups by their position in x . Then each group consists

of $N_y \times N_z$ cells which are attached in the topological y - and z -directions. For each cell in a group, the dice rule in 3D implies a relation between 4 barycenter values on 4 faces such that each of them is parallel to the topological xy - or zx -plane. Similarly to the 2D case, a collection of such relations from all cells in a group derives a single relation consisting of an alternating sum of $2N_y + 2N_z$ barycenter values on a set of boundary faces and it will be called a *strip* perpendicular to the topological x -axis. This induced relation on the strip is well-defined because the number of faces in the strip is always even. Figure 6.1 shows an example of a strip perpendicular to the topological x -axis. The signs on the strip represent the alternating sum of boundary barycenter values. For the topological x -direction, there are N_x strips perpendicular to the topological x -axis, and corresponding relations between barycenters on boundary faces. Repeating similar arguments for the topological y - and z -directions, we can find totally $N_x + N_y + N_z$ strips and corresponding relations between boundary barycenters.

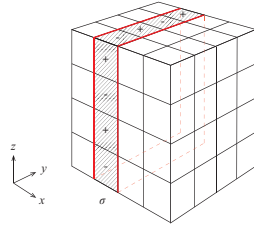


FIG. 6.1. An example of a strip

However, these induced relations are linearly independent. Choose an element K from one of corners in \mathcal{T}_h . There are three strips σ_K^x , σ_K^y , σ_K^z which are attached to K , and topologically perpendicular to the x -, y -, z -axes, respectively. Let us call each of these strips *the standard strip* for each axis. There are two options to assign proper alternating signs to barycenter values on each standard strip in order to make a corresponding alternating relation between boundary barycenters. For each standard strip, we choose an option for alternating sign in the relation to cancel out all boundary barycenters which belong to K when summing up all three relations on three standard strips. We will call them *the standard choices*. Consider σ , a strip among others, which is obviously parallel to one of these standard strips, without loss of generality, σ_K^x . There are also two options for alternating sign in the relation on σ . One option is same to the standard choice on σ_K^x : in this option, the sign for each boundary barycenter on σ is equal to the sign for the corresponding boundary barycenter in the standard choice on σ_K^x . The other option is just opposite to the standard choice. We make a choice on σ depending on the distance from σ_K^x . If σ is adjacent to σ_K^x , or is away from σ_K^x by an even number of faces in the topological x -direction, then we choose an option for alternating sign on σ to be opposite to the standard choice on σ_K^x . If σ is away from σ_K^x by an odd number of faces in the topological x -direction, then the same alternating sign as the standard choice is chosen on σ . Under this rule, we can make all choices for alternating sign in the induced relations on all $N_x + N_y + N_z$ strips. And it can be easily shown that the sum of all induced relations on all strips with chosen alternating sign becomes a trivial relation. It implies that there is a single linear relation between those induced relations on all strips. Therefore,

$$\#(\text{minimally essential discrete BCs})$$

$$\begin{aligned}
&= \#(\text{boundary faces}) - \#(\text{independent relations}) \\
&= 2(N_x N_y + N_y N_z + N_z N_x) - (N_x + N_y + N_z - 1). \quad \square
\end{aligned}$$

Depending on the evenness of N_x, N_y , and N_z , we have the following result on the dimension of periodic finite element space.

PROPOSITION 6.3. (*Periodic BC in 3D*) *In the case of periodic BC, we have*

$$\begin{aligned}
&\#(\text{minimally essential discrete BCs}) \\
&= (N_x N_y + N_y N_z + N_z N_x) \\
&\quad - [N_x \mathbf{e}(N_y) \mathbf{e}(N_z) + N_y \mathbf{e}(N_x) \mathbf{e}(N_z) + N_z \mathbf{e}(N_x) \mathbf{e}(N_y) - \mathbf{e}(N_x) \mathbf{e}(N_y) \mathbf{e}(N_z)],
\end{aligned}$$

and

$$\begin{aligned}
\dim V_{\#}^h = N_x N_y N_z - [N_x \mathbf{e}(N_y) \mathbf{e}(N_z) + N_y \mathbf{e}(N_x) \mathbf{e}(N_z) + N_z \mathbf{e}(N_x) \mathbf{e}(N_y) \\
- \mathbf{e}(N_x) \mathbf{e}(N_y) \mathbf{e}(N_z)].
\end{aligned}$$

Proof. Due to the same reason discussed in the 2D case, an induced relation between boundary barycenter values on a strip perpendicular to the x -axis can help to impose the periodic BC only when both N_y and N_z are even. In this case, coincidence of two barycenter values of the last boundary face pair is naturally achieved by pairwise coincidence of barycenter values of other boundary face pairs in the strip. Consequently, totally N_x periodic BCs can hold naturally due to other periodic BCs and induced boundary relations on strips perpendicular to the x -axis. Similar claims hold for induced boundary relations on strips topologically perpendicular to y -, and z -directional axes.

However, as discussed in the case of Dirichlet BC, due to the linear dependence between $N_x + N_y + N_z$ induced relations on all strips we have to consider 1 redundant relation when all $N_x + N_y + N_z$ strips are taken into account of *i.e.*, all N_x, N_y and N_z are even. This completes the proof. \square

6.2. Linear dependence of \mathfrak{B} in 3D. In this section, we identify a global coefficient representation for node-based functions in \mathfrak{B} with a vector in $\mathbb{R}^{|\mathfrak{B}|}$. With this identification, we use a vector $\mathbf{c} \in \mathbb{R}^{|\mathfrak{B}|}$ to represent a global coefficient representation on given 3D grid \mathcal{T}_h . In this sense, we denote the local coefficients of \mathbf{c} in $Q \in \mathcal{T}_h$ by $\mathbf{c}|_Q$. For the sake of simple description, we use this abusive notation as long as there is no chance of misunderstanding. A surjective linear map $B_h^{\mathfrak{B}} : \mathbb{R}^{|\mathfrak{B}|} \rightarrow V_{\#}^{\mathfrak{B},h}$ defined in Section 4 is obviously extended to the 3D case.

As shown in Figure 6.2, there are exactly 4 kinds of local coefficient representation for the zero function in a single element. The value at each vertex represents the coefficient for the corresponding node-based function in \mathfrak{B} . If any global coefficient representation for the zero function is restricted in an element, then it has to be a linear combination of these 4 elementary representations which are denoted by $\mathcal{A}, \mathcal{X}, \mathcal{Y}$ and \mathcal{Z} , respectively. In other words, any global representation for the zero function is obtained by a consecutive extension of local representation in an appropriate way.

For $D = \mathcal{A}, \mathcal{X} \cup \mathcal{A}, \mathcal{Y} \cup \mathcal{A}, \mathcal{Z} \cup \mathcal{A}, \mathcal{X} \cup \mathcal{Y} \cup \mathcal{Z} \cup \mathcal{A}$, designate \mathcal{S}_D the following subspace consisting of global representation:

$$\mathcal{S}_D := \left\{ \mathbf{c} \in \mathbb{R}^{|\mathfrak{B}|} \mid \mathbf{c}|_Q \in \text{Span}\{\mathcal{D}\} \forall Q \in \mathcal{T}_h \right\}.$$

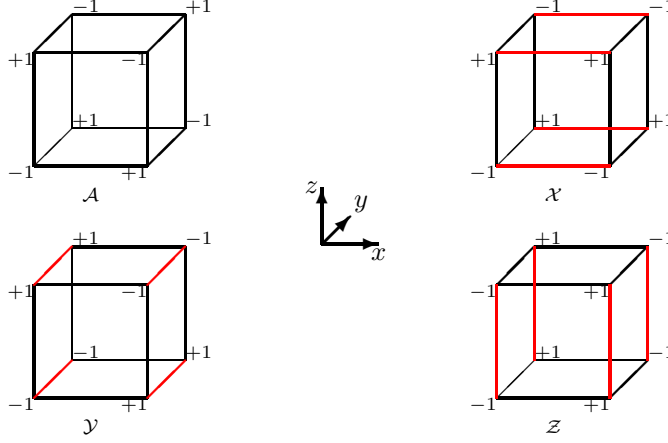


FIG. 6.2. Nontrivial representations for the zero function in an element: \mathcal{A} , \mathcal{X} , \mathcal{Y} , \mathcal{Z}

Remark 6.4. The definition of $B_h^{\mathfrak{B}}$ implies $\ker B_h^{\mathfrak{B}} = \mathcal{S}_{\mathcal{X} \cup \mathcal{Y} \cup \mathcal{Z} \cup \mathcal{A}}$.

We then have the following matching conditions on every face which is shared by two adjacent elements.

LEMMA 6.5. *Let $\mathbf{c} \in \mathcal{S}_{\mathcal{X} \cup \mathcal{Y} \cup \mathcal{Z} \cup \mathcal{A}}$, and $c_{ijk}^{\mathcal{X}}, c_{ijk}^{\mathcal{Y}}, c_{ijk}^{\mathcal{Z}}, c_{ijk}^{\mathcal{A}}$ denote coefficients of \mathbf{c} in an element $Q_{ijk} \in \mathcal{T}_h$ for $\mathcal{X}, \mathcal{Y}, \mathcal{Z}, \mathcal{A}$, respectively, i.e., $\mathbf{c}|_{Q_{ijk}} = c_{ijk}^{\mathcal{X}}\mathcal{X} + c_{ijk}^{\mathcal{Y}}\mathcal{Y} + c_{ijk}^{\mathcal{Z}}\mathcal{Z} + c_{ijk}^{\mathcal{A}}\mathcal{A}$. Then for all $1 \leq i \leq N_x, 1 \leq j \leq N_y, 1 \leq k \leq N_z$,*

$$c_{ijk}^{\mathcal{X}} - c_{ijk}^{\mathcal{A}} = c_{(i+1)jk}^{\mathcal{X}} + c_{(i+1)jk}^{\mathcal{A}}, \quad c_{ijk}^{\mathcal{Y}} = -c_{(i+1)jk}^{\mathcal{Y}}, \quad c_{ijk}^{\mathcal{Z}} = -c_{(i+1)jk}^{\mathcal{Z}}, \quad (6.2a)$$

$$c_{ijk}^{\mathcal{Y}} - c_{ijk}^{\mathcal{A}} = c_{i(j+1)k}^{\mathcal{Y}} + c_{i(j+1)k}^{\mathcal{A}}, \quad c_{ijk}^{\mathcal{Z}} = -c_{i(j+1)k}^{\mathcal{Z}}, \quad c_{ijk}^{\mathcal{X}} = -c_{i(j+1)k}^{\mathcal{X}}, \quad (6.2b)$$

$$c_{ijk}^{\mathcal{Z}} - c_{ijk}^{\mathcal{A}} = c_{ij(k+1)}^{\mathcal{Z}} + c_{ij(k+1)}^{\mathcal{A}}; \quad c_{ijk}^{\mathcal{X}} = -c_{ij(k+1)}^{\mathcal{X}}; \quad c_{ijk}^{\mathcal{Y}} = -c_{ij(k+1)}^{\mathcal{Y}}. \quad (6.2c)$$

Here all indices are understood up to modulo N_x, N_y, N_z , respectively, due to periodicity.

Remark 6.6. Conversely, local relations (6.2a)–(6.2c) in Lemma 6.5 for all $1 \leq i \leq N_x, 1 \leq j \leq N_y, 1 \leq k \leq N_z$ imply the well-definedness of $\mathbf{c} \in \mathcal{S}_{\mathcal{X} \cup \mathcal{Y} \cup \mathcal{Z} \cup \mathcal{A}}$, i.e., on each face shared by two adjacent elements the vertex values are matching.

Proof of Lemma 6.5. Two elements Q_{ijk} and $Q_{(i+1)jk}$ are adjacent in the topological x -direction, and sharing a common face topologically perpendicular to the x -axis. Thus the vertex values on the right face of the topologically left element Q_{ijk} have to be matched with the vertex values on the the topologically left face of the topologically right element $Q_{(i+1)jk}$. Since there are 4 nodes in the common face, we have 4 equations in 8 variables:

$$-c_{ijk}^{\mathcal{X}} + c_{ijk}^{\mathcal{Y}} + c_{ijk}^{\mathcal{Z}} + c_{ijk}^{\mathcal{A}} = -c_{(i+1)jk}^{\mathcal{X}} - c_{(i+1)jk}^{\mathcal{Y}} - c_{(i+1)jk}^{\mathcal{Z}} - c_{(i+1)jk}^{\mathcal{A}}, \quad (6.3a)$$

$$c_{ijk}^{\mathcal{X}} + c_{ijk}^{\mathcal{Y}} - c_{ijk}^{\mathcal{Z}} - c_{ijk}^{\mathcal{A}} = c_{(i+1)jk}^{\mathcal{X}} - c_{(i+1)jk}^{\mathcal{Y}} + c_{(i+1)jk}^{\mathcal{Z}} + c_{(i+1)jk}^{\mathcal{A}}, \quad (6.3b)$$

$$c_{ijk}^{\mathcal{X}} - c_{ijk}^{\mathcal{Y}} + c_{ijk}^{\mathcal{Z}} - c_{ijk}^{\mathcal{A}} = c_{(i+1)jk}^{\mathcal{X}} + c_{(i+1)jk}^{\mathcal{Y}} - c_{(i+1)jk}^{\mathcal{Z}} + c_{(i+1)jk}^{\mathcal{A}}, \quad (6.3c)$$

$$-c_{ijk}^{\mathcal{X}} - c_{ijk}^{\mathcal{Y}} - c_{ijk}^{\mathcal{Z}} + c_{ijk}^{\mathcal{A}} = -c_{(i+1)jk}^{\mathcal{X}} + c_{(i+1)jk}^{\mathcal{Y}} + c_{(i+1)jk}^{\mathcal{Z}} - c_{(i+1)jk}^{\mathcal{A}}. \quad (6.3d)$$

Simple calculation shows that (6.3) are equivalent to (6.2a). Similarly, considering faces topologically perpendicular to the y - and z -directions, we get (6.2b) and (6.2c), respectively. \square

The next decomposition theorem is essential for the dimension analysis in the 3D case.

THEOREM 6.7 (Decomposition Theorem). *The quotient space $\mathcal{S}_{\mathcal{X}\cup\mathcal{Y}\cup\mathcal{Z}\cup\mathcal{A}}/\mathcal{S}_{\mathcal{A}}$ can be decomposed as*

$$\mathcal{S}_{\mathcal{X}\cup\mathcal{Y}\cup\mathcal{Z}\cup\mathcal{A}}/\mathcal{S}_{\mathcal{A}} = \mathcal{S}_{\mathcal{X}\cup\mathcal{A}}/\mathcal{S}_{\mathcal{A}} \oplus \mathcal{S}_{\mathcal{Y}\cup\mathcal{A}}/\mathcal{S}_{\mathcal{A}} \oplus \mathcal{S}_{\mathcal{Z}\cup\mathcal{A}}/\mathcal{S}_{\mathcal{A}}. \quad (6.4)$$

Proof. It is clear that $\mathcal{S}_{\mathcal{A}} \subset \mathcal{S}_{\mathcal{X}\cup\mathcal{A}}, \mathcal{S}_{\mathcal{Y}\cup\mathcal{A}}, \mathcal{S}_{\mathcal{Z}\cup\mathcal{A}} \subset \mathcal{S}_{\mathcal{X}\cup\mathcal{Y}\cup\mathcal{Z}\cup\mathcal{A}}$ and $\mathcal{S}_{\mathcal{X}\cup\mathcal{A}} \cap \mathcal{S}_{\mathcal{Y}\cup\mathcal{A}} = \mathcal{S}_{\mathcal{Y}\cup\mathcal{A}} \cap \mathcal{S}_{\mathcal{Z}\cup\mathcal{A}} = \mathcal{S}_{\mathcal{Z}\cup\mathcal{A}} \cap \mathcal{S}_{\mathcal{X}\cup\mathcal{A}} = \mathcal{S}_{\mathcal{A}}$. Thus it is enough to show that for any $\mathbf{c} \in \mathcal{S}_{\mathcal{X}\cup\mathcal{Y}\cup\mathcal{Z}\cup\mathcal{A}}$, there exist $\mathbf{u} \in \mathcal{S}_{\mathcal{X}\cup\mathcal{A}}, \mathbf{v} \in \mathcal{S}_{\mathcal{Y}\cup\mathcal{A}}, \mathbf{w} \in \mathcal{S}_{\mathcal{Z}\cup\mathcal{A}}$ such that $\mathbf{c} \in \mathbf{u} + \mathbf{v} + \mathbf{w} + \mathcal{S}_{\mathcal{A}}$.

Let $c_{ijk}^{\mathcal{X}}, c_{ijk}^{\mathcal{Y}}, c_{ijk}^{\mathcal{Z}}, c_{ijk}^{\mathcal{A}}$ denote the coefficients of \mathbf{c} in $Q_{ijk} \in \mathcal{T}_h$ for $\mathcal{X}, \mathcal{Y}, \mathcal{Z}, \mathcal{A}$, respectively, i.e., $\mathbf{c}|_{Q_{ijk}} = c_{ijk}^{\mathcal{X}}\mathcal{X} + c_{ijk}^{\mathcal{Y}}\mathcal{Y} + c_{ijk}^{\mathcal{Z}}\mathcal{Z} + c_{ijk}^{\mathcal{A}}\mathcal{A}$. Due to Lemma 6.5, the relations (6.2a)–(6.2c) hold. Now we construct \mathbf{u}, \mathbf{v} , and \mathbf{w} . First, define $\mathbf{u} \in \mathbb{R}^{|\mathfrak{B}|}$ by

$$\mathbf{u}|_{Q_{ijk}} := u_{ijk}^{\mathcal{X}}\mathcal{X} + u_{ijk}^{\mathcal{A}}\mathcal{A} \quad \text{where} \quad u_{ijk}^{\mathcal{X}} = c_{ijk}^{\mathcal{X}}, u_{ijk}^{\mathcal{A}} = (-1)^{j+k}c_{i11}^{\mathcal{A}}. \quad (6.5)$$

We have $u_{ijk}^{\mathcal{Y}} = u_{ijk}^{\mathcal{Z}} = 0$. We can check the followings.

1. \mathbf{u} is well-defined, and belongs to $\mathcal{S}_{\mathcal{X}\cup\mathcal{Y}\cup\mathcal{Z}\cup\mathcal{A}}$: See Remark 6.6. For a face shared by two adjacent elements Q_{ijk} and $Q_{(i+1)jk}$,

$$\begin{aligned} u_{ijk}^{\mathcal{X}} - u_{(i+1)jk}^{\mathcal{A}} &= c_{ijk}^{\mathcal{X}} - (-1)^{j+k}c_{i11}^{\mathcal{A}} \\ &= c_{(i+1)jk}^{\mathcal{X}} + (-1)^{j+k}c_{(i+1)11}^{\mathcal{A}} = u_{(i+1)jk}^{\mathcal{X}} + u_{(i+1)jk}^{\mathcal{A}}. \end{aligned}$$

Thus \mathbf{u} is matching on all faces perpendicular to the x -axis. For the faces perpendicular to the y -axis, we have

$$\begin{aligned} u_{ijk}^{\mathcal{X}} &= c_{ijk}^{\mathcal{X}} = -c_{i(j+1)k}^{\mathcal{X}} = -u_{i(j+1)k}^{\mathcal{X}}, \\ -u_{ijk}^{\mathcal{A}} &= -(-1)^{j+k}c_{i11}^{\mathcal{A}} = (-1)^{j+1+k}c_{i11}^{\mathcal{A}} = u_{i(j+1)k}^{\mathcal{A}}, \end{aligned}$$

and similar for the faces perpendicular to the z -axis. Therefore \mathbf{u} is also matching along the y - and z -directions.

2. $\mathbf{u} \in \mathcal{S}_{\mathcal{X}\cup\mathcal{A}}$: It is trivial due to the definition of \mathbf{u} and $\mathcal{S}_{\mathcal{X}\cup\mathcal{A}}$.

Similarly to \mathbf{u} , we define \mathbf{v} and $\mathbf{w} \in \mathbb{R}^{|\mathfrak{B}|}$ by

$$\begin{aligned} \mathbf{v}|_{Q_{ijk}} &:= v_{ijk}^{\mathcal{Y}}\mathcal{Y} + v_{ijk}^{\mathcal{A}}\mathcal{A} \quad \text{where} \quad v_{ijk}^{\mathcal{Y}} = c_{ijk}^{\mathcal{Y}}, v_{ijk}^{\mathcal{A}} = (-1)^{i+k}c_{1j1}^{\mathcal{A}}, \\ \mathbf{w}|_{Q_{ijk}} &:= w_{ijk}^{\mathcal{Z}}\mathcal{Z} + w_{ijk}^{\mathcal{A}}\mathcal{A} \quad \text{where} \quad w_{ijk}^{\mathcal{Z}} = c_{ijk}^{\mathcal{Z}}, w_{ijk}^{\mathcal{A}} = (-1)^{i+j}c_{11k}^{\mathcal{A}}. \end{aligned}$$

Then both \mathbf{v} and \mathbf{w} are well-defined, and $\mathbf{v} \in \mathcal{S}_{\mathcal{Y}\cup\mathcal{A}}, \mathbf{w} \in \mathcal{S}_{\mathcal{Z}\cup\mathcal{A}}$. Thus $\mathbf{c} - (\mathbf{u} + \mathbf{v} + \mathbf{w}) \in \mathcal{S}_{\mathcal{X}\cup\mathcal{Y}\cup\mathcal{Z}\cup\mathcal{A}}$. We can conclude $\mathbf{c} - (\mathbf{u} + \mathbf{v} + \mathbf{w}) \in \mathcal{S}_{\mathcal{A}}$ since for each Q_{ijk} ,

$$\mathbf{c} - (\mathbf{u} + \mathbf{v} + \mathbf{w})|_{Q_{ijk}} = (c_{ijk}^{\mathcal{A}} - (-1)^{j+k}c_{i11}^{\mathcal{A}} - (-1)^{i+k}c_{1j1}^{\mathcal{A}} - (-1)^{i+j}c_{11k}^{\mathcal{A}})\mathcal{A}. \quad \square$$

COROLLARY 6.8. $\dim \ker B_h^{\mathfrak{B}} = \dim \mathcal{S}_{\mathcal{X}\cup\mathcal{A}} + \dim \mathcal{S}_{\mathcal{Y}\cup\mathcal{A}} + \dim \mathcal{S}_{\mathcal{Z}\cup\mathcal{A}} - 2 \dim \mathcal{S}_{\mathcal{A}}$.

The following lemmas explain the dimension of subspaces which depends on parity of the discretization numbers.

LEMMA 6.9. (The dimension of $\mathcal{S}_{\mathcal{X}\cup\mathcal{A}}$, $\mathcal{S}_{\mathcal{Y}\cup\mathcal{A}}$, $\mathcal{S}_{\mathcal{Z}\cup\mathcal{A}}$)

$$\dim \mathcal{S}_{\mathcal{X}\cup\mathcal{A}} = N_x \mathfrak{e}(N_y) \mathfrak{e}(N_z), \quad (6.6a)$$

$$\dim \mathcal{S}_{\mathcal{Y}\cup\mathcal{A}} = \mathfrak{e}(N_x) N_y \mathfrak{e}(N_z), \quad (6.6b)$$

$$\dim \mathcal{S}_{\mathcal{Z}\cup\mathcal{A}} = \mathfrak{e}(N_x) \mathfrak{e}(N_y) N_z. \quad (6.6c)$$

Proof. It is enough to show the claim for $\mathcal{S}_{\mathcal{X}\cup\mathcal{A}}$, since the others are similar. Let $\mathbf{c} \in \mathcal{S}_{\mathcal{X}\cup\mathcal{A}}$ where $\mathbf{c}|_{Q_{ijk}} = c_{ijk}^{\mathcal{X}} \mathcal{X} + c_{ijk}^{\mathcal{A}} \mathcal{A}$ in each cube $Q_{ijk} \in \mathcal{T}_h$. By applying the matching conditions (6.2b) and (6.2c) consecutively, it can be shown

$$c_{ijk}^{\mathcal{X}} = (-1)^{j+k} c_{i11}^{\mathcal{X}} \quad \text{and} \quad c_{ijk}^{\mathcal{A}} = (-1)^{j+k} c_{i11}^{\mathcal{A}}.$$

Consider $N_x + 1$ combined surfaces such that each of them consists of $N_y \times N_z$ faces in \mathcal{T}_h , and is lying on the same hyperplane perpendicular to the x -axis. The above relations imply that on each surface the coefficients for node-based functions are all the same, but with alternating sign like a checkerboard pattern at nodes, not on faces. Due to the identification between boundary nodes in the y - and z -directions, all coefficients vanish unless both N_y and N_z are even.

Under the case of even N_y and N_z , we consider a basis checkerboard pattern at nodes on a combined surface consisting of $+1$ and -1 , alternatively, as Figure 6.3 (a) shows. In the figure, the plus and minus sign at nodes represent the positive value one, and the negative value one, respectively. We get $N_x + 1$ checkerboard patterns on $N_x + 1$ combined surfaces in series (Figure 6.3 (b)). Based on the basis checkerboard pattern described above, we can represent all coefficients on each combined surface by a single factor in real number. Due to the identification between boundary nodes in the x -direction, factors for the first and the last combined surface must be same. Then the series of $N_x + 1$ checkerboard patterns compose a global representation for a function in $\mathcal{S}_{\mathcal{X}\cup\mathcal{A}}$ (Figure 6.3 (c)). Conversely, for the $N_x + 1$ combined surfaces which are perpendicular to the x -axis and the basis checkerboard pattern at nodes on surfaces, suppose $N_x + 1$ factors are given, where the first and the last of them are same. Then we can determine unique $c_{ijk}^{\mathcal{X}}$ and $c_{ijk}^{\mathcal{A}}$, for all $Q_{ijk} \in \mathcal{T}_h$. Therefore, only in the case when both N_y and N_z are even, $\mathcal{S}_{\mathcal{X}\cup\mathcal{A}}$ is equivalent to $\{\mathbf{v} \in \mathbb{R}^{N_x+1} \mid v_1 = v_{N_x+1}\}$ and $\dim \mathcal{S}_{\mathcal{X}\cup\mathcal{A}} = N_x$ consequently. \square

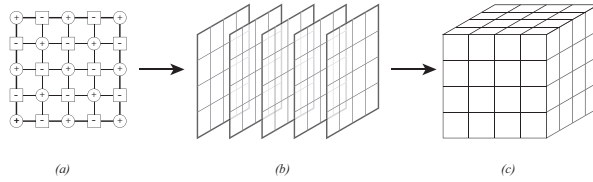


FIG. 6.3. Construction of a global representation for a function in $\mathcal{S}_{\mathcal{X}\cup\mathcal{A}}$

LEMMA 6.10. (The dimension of $\mathcal{S}_{\mathcal{A}}$)

$$\dim \mathcal{S}_{\mathcal{A}} = \mathfrak{e}(N_x) \mathfrak{e}(N_y) \mathfrak{e}(N_z). \quad (6.7)$$

Proof. Let $\mathbf{c} \in \mathcal{S}_{\mathcal{A}}$ where $\mathbf{c}|_{Q_{ijk}} = c_{ijk}^{\mathcal{A}} \mathcal{A}$ in each cube Q_{ijk} . By applying the matching conditions (6.2a)–(6.2c) consecutively, it is shown $c_{ijk}^{\mathcal{A}} = (-1)^{i+j+k+1} c_{111}^{\mathcal{A}}$. Due to the identification of boundary nodes in the x -, y -, and z -directions, all coefficients vanish unless all N_x , N_y and N_z are even. In the case of all even N_x , N_y

and N_z , it is easily shown that the coefficients form a multiple of *the 3D checkerboard pattern* at nodes. Therefore $\dim \mathcal{S}_A = 1$. \square

The following proposition is a direct consequence of Corollary 6.8, Lemmas 6.9 and 6.10.

PROPOSITION 6.11. (*The dimensions of $\ker B_h^{\mathfrak{B}}$, $V_{\#}^{\mathfrak{B},h}$ in 3D*)

$$\begin{aligned} \dim \ker B_h^{\mathfrak{B}} &= N_x \mathfrak{e}(N_y) \mathfrak{e}(N_z) + \mathfrak{e}(N_x) N_y \mathfrak{e}(N_z) + \mathfrak{e}(N_x) \mathfrak{e}(N_y) N_z - 2\mathfrak{e}(N_x) \mathfrak{e}(N_y) \mathfrak{e}(N_z), \\ \dim V_{\#}^{\mathfrak{B},h} &= N_x N_y N_z - [N_x \mathfrak{e}(N_y) \mathfrak{e}(N_z) + \mathfrak{e}(N_x) N_y \mathfrak{e}(N_z) + \mathfrak{e}(N_x) \mathfrak{e}(N_y) N_z \\ &\quad - 2\mathfrak{e}(N_x) \mathfrak{e}(N_y) \mathfrak{e}(N_z)]. \end{aligned}$$

6.3. A basis for $V_{\#}^h$ in 3D. Propositions 6.3 and 6.11 imply that $V_{\#}^{\mathfrak{B},h}$ is a proper subset of $V_{\#}^h$ if at most one of N_x , N_y , and N_z is odd. Furthermore, if all N_x , N_y , and N_z are even, then there exist $2(N_x + N_y + N_z) - 3$ complementary basis functions for $V_{\#}^h$, not belonging to $V_{\#}^{\mathfrak{B},h}$. If only N_l is odd, then the number of complementary basis functions for $V_{\#}^h$ is $2N_l$. In other cases, $V_{\#}^{\mathfrak{B},h}$ is equal to $V_{\#}^h$. We will discuss about the complementary basis functions below.

THEOREM 6.12. (*A complementary basis for $V_{\#}^h$ in 3D*) Suppose a rectangular domain Ω is given with a triangulation \mathcal{T}_h , consisting of cubes, in which the number of elements along coordinates are N_x , N_y , N_z . For given $1 \leq i \leq N_x$, let Ω_i^x be the subdomain consisting of $N_y \times N_z$ cubes whose discrete position in x -coordinate are all same to i . Let $(\psi_i^x)_y$ denote a piecewise linear function in $V_{\#}^h$, whose support is Ω_i^x , such that it has nonzero barycenter values only on faces perpendicular to the y -axis, and all the nonzero barycenter values are 1 with alternating sign in the y - and z -directions. We can consider $(\psi_i^x)_z$, $(\psi_j^y)_x$, $(\psi_j^y)_z$, $(\psi_k^z)_x$, $(\psi_k^z)_y$ in similar manner. The followings hold.

1. If all N_x , N_y , and N_z are even, then $V_{\#}^{\mathfrak{B},h}$ is a proper subset of $V_{\#}^h$. The union of
 - any $N_x + N_y - 1$ among $\mathfrak{A}_z := \{(\psi_i^x)_z, (\psi_j^y)_z\}_{1 \leq i \leq N_x, 1 \leq j \leq N_y}$,
 - any $N_y + N_z - 1$ among $\mathfrak{A}_x := \{(\psi_j^y)_x, (\psi_k^z)_x\}_{1 \leq j \leq N_y, 1 \leq k \leq N_z}$, and
 - any $N_z + N_x - 1$ among $\mathfrak{A}_y := \{(\psi_k^z)_y, (\psi_i^x)_y\}_{1 \leq i \leq N_x, 1 \leq k \leq N_z}$
is a complementary basis for $V_{\#}^h$, not belonging to $V_{\#}^{\mathfrak{B},h}$.
2. If only N_l is odd (and N_μ, N_ν are even), then $V_{\#}^{\mathfrak{B},h}$ is a proper subset of $V_{\#}^h$. Moreover, $\{(\psi_j^l)_\mu, (\psi_j^l)_\nu\}_{1 \leq j \leq N_l}$ is a complementary basis for $V_{\#}^h$, which is not contained in $V_{\#}^{\mathfrak{B},h}$.
3. Otherwise, $V_{\#}^{\mathfrak{B},h} = V_{\#}^h$.

Proof. For the first case, suppose that all N_x , N_y , and N_z are even. Note that all nonzero barycenter values of $(\psi_i^x)_y$ are lying on the faces perpendicular to only one axis with alternating sign, as similar to the alternating function ψ_x in the 2D case (Figure 6.4 (a), (b)), and its support is Ω_i^x (Figure 6.4 (c)). Using a similar argument as in the 2D case, it is easily shown that $(\psi_i^x)_y$ is well-defined, and not belonging to $V_{\#}^{\mathfrak{B},h}$ since N_y and N_z are even. A similar property holds for $(\psi_i^x)_z$, a piecewise linear function in $V_{\#}^h$ whose support is Ω_i^x and which has nonzero barycenter values as 1 only on faces perpendicular to the z -axis with alternating sign in the y - and z -directions. Thus there exist $2N_x$ alternating functions, $\{(\psi_i^x)_y, (\psi_i^x)_z\}_{1 \leq i \leq N_x}$, for $V_{\#}^h$ associated with strips perpendicular to the x -axis. By considering other strips perpendicular to the y - or z -axis, we can find out $2(N_x + N_y + N_z)$ alternating functions for $V_{\#}^h$, not belonging to $V_{\#}^{\mathfrak{B},h}$: $\{(\psi_i^x)_y, (\psi_i^x)_z, (\psi_j^y)_x, (\psi_j^y)_z, (\psi_k^z)_x, (\psi_k^z)_y\}_{1 \leq i \leq N_x, 1 \leq j \leq N_y, 1 \leq k \leq N_z}$.

However, there is a single relation between the alternating functions in each direction on subscript. An alternating sum of $(\psi_i^x)_z$ in $1 \leq i \leq N_x$ is equal to that of $(\psi_j^y)_z$ in $1 \leq j \leq N_y$. And any $N_x + N_y - 1$ among all $(\psi_i^x)_z$ and $(\psi_j^y)_z$ are linearly independent due to their supports. Similarly, any $N_y + N_z - 1$ among all $(\psi_j^y)_x$ and $(\psi_k^z)_x$ are linearly independent, and so any $N_z + N_x - 1$ among all $(\psi_k^z)_y$ and $(\psi_i^x)_y$ are. Consequently, suitably chosen $2(N_x + N_y + N_z) - 3$ alternating functions form a complementary basis for $V_{\#}^h$.

In the case of only one odd N_l (and even N_μ, N_ν), the set of all alternating functions associated to the strips perpendicular to the l -axis, $\{(\psi_j^t)_\mu, (\psi_j^t)_\nu\}_{1 \leq j \leq N_l}$, are meaningful because N_μ and N_ν are even. \square

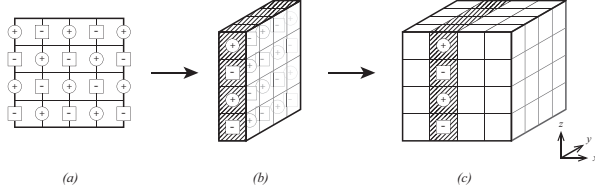


FIG. 6.4. Construction of an alternating function in 3D

6.4. Stiffness matrix associated with \mathfrak{B} in 3D. The stiffness matrix $\mathbf{S}_h^{\mathfrak{B}}$ associated with \mathfrak{B} is defined as in (4.5) but in 3D space. See Figure 6.5 for the 3D local stencil for the stiffness matrix associated with \mathfrak{B} . Propositions 4.5 and 6.11 lead the following proposition.

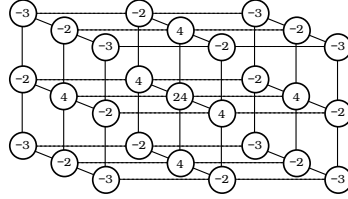


FIG. 6.5. The stencil for $\mathbf{S}_h^{\mathfrak{B}}$ with uniform cubes of size $h \times h \times h$ in 3D.

PROPOSITION 6.13. (The dimension of $\ker \mathbf{S}_h^{\mathfrak{B}}$ in 3D)

$$\dim \ker \mathbf{S}_h^{\mathfrak{B}} = N_x \mathfrak{e}(N_y) \mathfrak{e}(N_z) + \mathfrak{e}(N_x) N_y \mathfrak{e}(N_z) + \mathfrak{e}(N_x) \mathfrak{e}(N_y) N_z - 2 \mathfrak{e}(N_x) \mathfrak{e}(N_y) \mathfrak{e}(N_z) + 1.$$

Let us assemble $\mathbf{S}_h^{\mathfrak{B}}$ for various combinations of N_x, N_y , and N_z . The rank deficiency is computed by using MATLAB. Table 6.1 shows numerically obtained rank deficiency of $\mathbf{S}_h^{\mathfrak{B}}$ in 3D space. Without loss of generality, it only represents combinations which hold $N_x \geq N_y \geq N_z$. Numbers in red, blue, and black represent the case of all even discretizations and the case of odd discretization in only one direction, and the other cases, respectively. These results imply that the rank deficiency pattern depend on parity combination and confirm our theoretical result in Proposition 6.13.

6.5. Numerical schemes in 3D. Consider again an elliptic problem with periodic BC (5.1) with the compatibility condition $\int_{\Omega} f = 0$, the corresponding weak formulation (5.1), and the corresponding discrete weak formulation (5.2) in 3D.

Throughout this section, we assume that all N_x, N_y , and N_z are even.

$N_z = 2$		N_y						$N_z = 3$									
		2	3	4	5	6	7	8			2	3	4	5	6	7	8
N_x	2	5								2							
	3	4	1							3	1						
	4	7	4	9						4	1	4					
	5	6	1	6	1					5	1	1	1				
	6	9	4	11	6	13				6	1	4	1	4			
	7	8	1	8	1	8	1			7	1	1	1	1	1		
	8	11	4	13	6	15	8	17		8	1	4	1	4	1	4	
	$N_z = 4$		N_y							$N_z = 5$							
		2	3	4	5	6	7	8			2	3	4	5	6	7	8
	2									2							
	3									3							
	4			11						4							
	5			6	1					5			1				
	6			13	6	15				6			1	6			
	7			8	1	8	1			7			1	1	1		
	8			15	6	17	8	19		8			1	6	1	6	

TABLE 6.1
Numerically obtained rank deficiency of $\mathbf{S}_h^{\mathfrak{B}}$ in 3D

Additional Notations & Properties. \mathfrak{B}^b again denotes a basis for $V_{\#}^{\mathfrak{B},h}$, a proper subset of \mathfrak{B} . A constructive method for \mathfrak{B}^b will be given. Let \mathfrak{A} and \mathfrak{A}^b be the set of all alternating functions, and a complementary basis for $V_{\#}^h$ which consists of alternating functions as in Theorem 6.12, respectively. Without loss of generality, we may write $\mathfrak{B}^b = \{\phi_j\}_{j=1}^{|\mathfrak{B}^b|}$, $\mathfrak{B} = \{\phi_j\}_{j=1}^{|\mathfrak{B}|}$, $\mathfrak{A}^b = \{\psi_j\}_{j=1}^{|\mathfrak{A}^b|}$, and $\mathfrak{A} = \{\psi_j\}_{j=1}^{|\mathfrak{A}|}$. Define two extended sets $\mathfrak{E} := \mathfrak{B} \cup \mathfrak{A}$, and $\mathfrak{E}^b := \mathfrak{B}^b \cup \mathfrak{A}^b$. Even in the 3D case, \mathfrak{E}^b forms a basis for $V_{\#}^h$. The characteristics of \mathfrak{B}^b , \mathfrak{B} , \mathfrak{E}^b , and \mathfrak{E} in 3D are summarized in Table 6.2.

\mathcal{S}	$ \mathcal{S} $	Span \mathcal{S}	dim Span \mathcal{S}
\mathfrak{B}^b	$N_x N_y N_z - (N_x + N_y + N_z) + 2$	$V_{\#}^{\mathfrak{B},h}$	$N_x N_y N_z - (N_x + N_y + N_z) + 2$
\mathfrak{B}	$N_x N_y N_z$	$V_{\#}^{\mathfrak{B},h}$	$N_x N_y N_z - (N_x + N_y + N_z) + 2$
\mathfrak{E}^b	$N_x N_y N_z + (N_x + N_y + N_z) - 1$	$V_{\#}^h$	$N_x N_y N_z + (N_x + N_y + N_z) - 1$
\mathfrak{E}	$N_x N_y N_z + 2(N_x + N_y + N_z)$	$V_{\#}^h$	$N_x N_y N_z + (N_x + N_y + N_z) - 1$

TABLE 6.2
Characteristic of each test and trial function set \mathcal{S} in 3D when all N_x, N_y, N_z are even

Remark 6.14. Unlike in the 2D case, \mathfrak{A} may not be linearly independent in the 3D case. Thus we use \mathfrak{A}^b , a linearly independent subset, instead of \mathfrak{A} to construct \mathfrak{E}^b as a basis for $V_{\#}^h$.

LEMMA 6.15. *Let \mathfrak{B} and \mathfrak{A} be as above. Then the followings hold.*

1. $a_h(\phi, \psi) = 0 \forall \phi \in \mathfrak{B} \forall \psi \in \mathfrak{A}$.
2. $\int_{\Omega} \psi = 0 \forall \psi \in \mathfrak{A}$.
3. *There exists an h -independent constant C such that $\|\psi\|_0 \leq Ch^{1/2}$ and $|\psi|_{1,h} \leq Ch^{-1/2} \forall \psi \in \mathfrak{A}$.*

Remark 6.16. The second equation in Lemma 5.2 does not hold in the 3D case. If $\mu = \nu$, then $a_h((\psi^\mu)_\mu, (\psi^\nu)_\nu)$ does not vanish in general.

For the 3D case, we define again $\mathbf{S}_h^{\mathfrak{B}^b}$, $\tilde{\mathbf{S}}_h^{\mathfrak{B}^b}$, and $\mathbf{S}_h^{\mathfrak{A}}$ as in (5.3)–(5.5), respectively. Furthermore we define $\mathbf{S}_h^{\mathfrak{A}^b}$, the stiffness matrix associated with \mathfrak{A}^b similarly. Define

the linear systems $\tilde{\mathcal{L}}_h^{\mathfrak{E}^b}, \mathcal{L}_h^{\mathfrak{E}^b}$ as in (5.7), (5.8), with slight modification since \mathfrak{E}^b is equal to $\mathfrak{B}^b \cup \mathfrak{A}^b$ in the 3D case. Other linear systems $\mathcal{L}_h^{\mathfrak{E}}, \mathcal{L}_h^{\mathfrak{B}}$ are defined as in (5.12), (5.14). The solutions $\tilde{\mathbf{u}}^b, \mathbf{u}^b, \mathbf{u}^{\natural}, \bar{\mathbf{u}}^{\natural}$, and the numerical solutions $u_h, u_h^b, u_h^{\natural}, \bar{u}_h^{\natural}$ are defined as in (5.7)–(5.9), (5.12)–(5.14), (5.6), (5.10), (5.11), (5.15).

The following describes relations between numerical solutions in 3D, as an analog of Theorem 5.3.

THEOREM 6.17. *Let $(\mathcal{T}_h)_{0 < h}$ be a family of uniform rectangular decomposition, that is, $\mathcal{T}_h = \tilde{\mathcal{T}}_h$ for all h . Assume that N_x, N_y and N_z are even. Let $u_h, u_h^b, u_h^{\natural}, \bar{u}_h^{\natural}$ be the numerical solutions of (5.1) in 3D as (5.6), (5.10), (5.11), (5.15), respectively, with $\mathfrak{E}^b = \mathfrak{B}^b \cup \mathfrak{A}^b$. Then $u_h = u_h^b = u_h^{\natural}$, and*

$$\|u_h^{\natural} - \bar{u}_h^{\natural}\|_0 \leq Ch^2 \|f\|_0, \quad |u_h^{\natural} - \bar{u}_h^{\natural}|_{1,h} \leq Ch \|f\|_0.$$

Proof. The equality between u_h and u_h^b can be proved as in the 2D case. Since \mathfrak{B}^b is a basis for $V_{\#}^{\mathfrak{B}^b, h}$, there exist $t_{\ell j} \in \mathbb{R}$ for $1 \leq \ell \leq |\mathfrak{B}| - |\mathfrak{B}^b|$ and $1 \leq j \leq |\mathfrak{B}^b|$, such that

$$\phi_{|\mathfrak{B}^b|+\ell} = \sum_{j=1}^{|\mathfrak{B}^b|} t_{\ell j} \phi_j. \quad (6.8)$$

Thus $\sum_{K \in \mathcal{T}_h} \nabla \phi_k \cdot \nabla \left(\phi_{|\mathfrak{B}^b|+\ell} - \sum_{j=1}^{|\mathfrak{B}^b|} t_{\ell j} \phi_j \right) = 0$ for all k , and it is simplified as $(\mathbf{S}_h^{\mathfrak{B}^b})_{|\mathfrak{B}^b|+\ell, k} = \sum_{j=1}^{|\mathfrak{B}^b|} t_{\ell j} (\mathbf{S}_h^{\mathfrak{B}^b})_{jk}$. Let \mathbf{T} denote a matrix of size $(|\mathfrak{B}| - |\mathfrak{B}^b|) \times |\mathfrak{B}^b|$ such that $(\mathbf{T})_{\ell j} = t_{\ell j}$. Then the last equation for $1 \leq \ell \leq |\mathfrak{B}| - |\mathfrak{B}^b|$ and $1 \leq k \leq |\mathfrak{B}^b|$ can be expressed as a linear system

$$[\mathbf{S}_h^{\mathfrak{B}^b}]_{|\mathfrak{B}^b|+1:|\mathfrak{B}|, 1:|\mathfrak{B}^b|} = \mathbf{T} [\mathbf{S}_h^{\mathfrak{B}^b}]_{1:|\mathfrak{B}^b|, 1:|\mathfrak{B}^b|}. \quad (6.9)$$

Note that $[\mathbf{S}_h^{\mathfrak{B}^b}]_{1:|\mathfrak{B}^b|, 1:|\mathfrak{B}^b|}$ is just equal to $\mathbf{S}_h^{\mathfrak{B}^b}$. Let $\begin{bmatrix} \mathbf{u}^b|_{\mathfrak{B}^b} \\ \mathbf{0} \end{bmatrix}$ be a trivial extension of $\mathbf{u}^b|_{\mathfrak{B}^b}$ into a vector in $\mathbb{R}^{|\mathfrak{B}^b|}$ by padding zeros. Then

$$\mathbf{S}_h^{\mathfrak{B}^b} \begin{bmatrix} \mathbf{u}^b|_{\mathfrak{B}^b} \\ \mathbf{0} \end{bmatrix} = \begin{bmatrix} \mathbf{S}_h^{\mathfrak{B}^b} \mathbf{u}^b|_{\mathfrak{B}^b} \\ [\mathbf{S}_h^{\mathfrak{B}^b}]_{|\mathfrak{B}^b|+1:|\mathfrak{B}|, 1:|\mathfrak{B}^b|} \mathbf{u}^b|_{\mathfrak{B}^b} \end{bmatrix} = \begin{bmatrix} \mathbf{S}_h^{\mathfrak{B}^b} \mathbf{u}^b|_{\mathfrak{B}^b} \\ \mathbf{T} \mathbf{S}_h^{\mathfrak{B}^b} \mathbf{u}^b|_{\mathfrak{B}^b} \end{bmatrix} = \begin{bmatrix} \int_{\Omega} f \mathfrak{B}^b \\ \mathbf{T} \int_{\Omega} f \mathfrak{B}^b \end{bmatrix}$$

since $\mathbf{S}_h^{\mathfrak{B}^b} \mathbf{u}^b|_{\mathfrak{B}^b} = \int_{\Omega} f \mathfrak{B}^b$. We can easily derive

$$\mathbf{T} \int_{\Omega} f \mathfrak{B}^b = \mathbf{T} \begin{bmatrix} \int_{\Omega} f \phi_1 \\ \vdots \\ \int_{\Omega} f \phi_{|\mathfrak{B}^b|} \end{bmatrix} = \begin{bmatrix} \int_{\Omega} f \sum_{j=1}^{|\mathfrak{B}^b|} t_{1j} \phi_j \\ \vdots \\ \int_{\Omega} f \sum_{j=1}^{|\mathfrak{B}^b|} t_{|\mathfrak{B}^b|j} \phi_j \end{bmatrix} = \begin{bmatrix} \int_{\Omega} f \phi_{|\mathfrak{B}^b|+1} \\ \vdots \\ \int_{\Omega} f \phi_{|\mathfrak{B}|} \end{bmatrix},$$

which implies $\mathbf{S}_h^{\mathfrak{B}^b} \begin{bmatrix} \mathbf{u}^b|_{\mathfrak{B}^b} \\ \mathbf{0} \end{bmatrix} = \int_{\Omega} f \mathfrak{B}$. In the same way we can obtain $\mathbf{S}_h^{\mathfrak{A}^b} \begin{bmatrix} \mathbf{u}^b|_{\mathfrak{A}^b} \\ \mathbf{0} \end{bmatrix} = \int_{\Omega} f \mathfrak{A}$, and these equations derive $u_h^{\natural} = u_h^b$ by the same argument as in the 2D case.

For the last, consider the difference between u_h^{\natural} and \bar{u}_h^{\natural} . We can easily observe that $u_h^{\natural} - \bar{u}_h^{\natural} = \mathbf{u}^{\natural}|_{\mathfrak{A}^b} \mathfrak{A}$, and $a_h(u_h^{\natural} - \bar{u}_h^{\natural}, \psi) = \int_{\Omega} f \psi$ for all $\psi \in \mathfrak{A}$. Thus

$$|u_h^{\natural} - \bar{u}_h^{\natural}|_{1,h}^2 = a_h \left(u_h^{\natural} - \bar{u}_h^{\natural}, u_h^{\natural} - \bar{u}_h^{\natural} \right)$$

$$= \int_{\Omega} f(u_h^{\natural} - \bar{u}_h^{\natural}) \leq C \|f\|_0 \|u_h^{\natural} - \bar{u}_h^{\natural}\|_0 = Ch \|f\|_0 |u_h^{\natural} - \bar{u}_h^{\natural}|_{1,h}$$

due to the following lemma, and we immediately obtain the difference in mesh-dependent norm, and in L^2 -norm. \square

LEMMA 6.18. *Let $\mathcal{M}_h^{\mathfrak{A}}$ be the mass matrix associated with \mathfrak{A} . Then there exists an h -independent constant C such that $\mathcal{M}_h^{\mathfrak{A}} = Ch^2 \mathcal{S}_h^{\mathfrak{A}}$. In a consequence, $\|v_h\|_0 = C^{1/2} h |v_h|_{1,h}$ for all $v_h \in \text{Span } \mathfrak{A}$.*

Proof. Remind that $(\psi_j^{\iota})_{\mu}$ is the alternating function such that the support is Ω_j^{ι} and the nonzero barycenter values are only lying on faces perpendicular to the μ -axis. Thus only μ -component of the piecewise gradient of $(\psi_j^{\iota})_{\mu}$ survives. It implies that $a_h((\psi_j^{\iota})_{\mu}, (\psi_k^{\lambda})_{\nu}) = 0$ if $\mu \neq \nu$. Therefore we can consider $\mathcal{S}_h^{\mathfrak{A}}$ as a block diagonal

$$\text{matrix: } \mathcal{S}_h^{\mathfrak{A}} = \begin{bmatrix} \mathcal{S}_h^{\mathfrak{A}_x} & \mathbf{0} & \mathbf{0} \\ \mathbf{0} & \mathcal{S}_h^{\mathfrak{A}_y} & \mathbf{0} \\ \mathbf{0} & \mathbf{0} & \mathcal{S}_h^{\mathfrak{A}_z} \end{bmatrix}, \text{ where } \mathfrak{A}_x, \mathfrak{A}_y, \mathfrak{A}_z \text{ are defined as in Theorem 6.12,}$$

and $\mathcal{S}_h^{\mathfrak{A}_x}, \mathcal{S}_h^{\mathfrak{A}_y}, \mathcal{S}_h^{\mathfrak{A}_z}$ are the stiffness matrices associated with the respective sets.

We can also consider $\mathcal{M}_h^{\mathfrak{A}}$ as a block diagonal matrix in the same structure, since the following observation: if $\mu \neq \lambda$, then

$$\begin{aligned} ((\psi_j^{\iota})_{\mu}, (\psi_k^{\lambda})_{\nu})_{\Omega} &= \int_{\Omega} (\psi_j^{\iota})_{\mu} (\psi_k^{\lambda})_{\nu} = \sum_{Q \in \mathcal{T}_h(\Omega)} \int_Q (\psi_j^{\iota})_{\mu} (\psi_k^{\lambda})_{\nu} \\ &= \sum_{Q \in \mathcal{T}_h(\Omega)} h \int_{Q_{\mu}} (\psi_j^{\iota})_{\mu} d\mu \int_{Q_{\nu}} (\psi_k^{\lambda})_{\nu} d\nu = 0. \end{aligned}$$

$$\text{Set } \mathcal{M}_h^{\mathfrak{A}} = \begin{bmatrix} \mathcal{M}_h^{\mathfrak{A}_x} & \mathbf{0} & \mathbf{0} \\ \mathbf{0} & \mathcal{M}_h^{\mathfrak{A}_y} & \mathbf{0} \\ \mathbf{0} & \mathbf{0} & \mathcal{M}_h^{\mathfrak{A}_z} \end{bmatrix}, \text{ where } \mathcal{M}_h^{\mathfrak{A}_x}, \mathcal{M}_h^{\mathfrak{A}_y}, \mathcal{M}_h^{\mathfrak{A}_z} \text{ are the mass matrices}$$

associated with the respective sets. Therefore, it is enough to show $\mathcal{M}_h^{\mathfrak{A}_{\mu}} = Ch^2 \mathcal{S}_h^{\mathfrak{A}_{\mu}}$ for each $\mu \in \{x, y, z\}$.

First, we consider the blocks associated with $\mathfrak{A}_x = \{(\psi_j^y)_x, (\psi_k^z)_x\}$ for $1 \leq j \leq N_y, 1 \leq k \leq N_z$. The proof for other blocks is similar. For any two alternating functions $(\psi_j^y)_x$ and $(\psi_k^z)_x$ in \mathfrak{A}_x , we have

Case 1. if $\iota = \lambda$ (let them be equal to y , without loss of generality), then

$$a_h((\psi_j^y)_x, (\psi_k^y)_x) = \sum_{Q \in \mathcal{T}_h(\Omega)} \int_Q \nabla(\psi_j^y)_x \cdot \nabla(\psi_k^y)_x = \sum_{Q \in \mathcal{T}_h(\Omega_j^y \cap \Omega_k^y)} \int_Q \frac{4}{h^2} = 4N_x N_z h \delta_{jk},$$

since the number of cubes in Ω_j^y is $N_x N_z$. Here, δ_{jk} denotes the Kronecker delta.

Case 2. if $\iota \neq \lambda$ (let $\iota = y$ and $\lambda = z$, without loss of generality), then

$$a_h((\psi_j^y)_x, (\psi_k^z)_x) = \sum_{Q \in \mathcal{T}_h(\Omega)} \int_Q \nabla(\psi_j^y)_x \cdot \nabla(\psi_k^z)_x = \sum_{Q \in \mathcal{T}_h(\Omega_j^y \cap \Omega_k^z)} \int_Q \frac{4}{h^2} = 4N_x h,$$

since the number of cubes in $\Omega_j^y \cap \Omega_k^z$ is N_x . On the other hand, it is ready to see that

$$((\psi_j^y)_x, (\psi_k^y)_x)_{\Omega} = \sum_{Q \in \mathcal{T}_h(\Omega_j^y \cap \Omega_k^y)} \int_Q (\psi_j^y)_x (\psi_k^y)_x = \frac{N_x N_z h^3 \delta_{jk}}{3},$$

and

$$((\psi_j^y)_x, (\psi_k^z)_x)_\Omega = \sum_{Q \in \mathcal{T}_h(\Omega_j^y \cap \Omega_k^z)} \int_Q (\psi_j^y)_x (\psi_k^z)_x = \frac{N_x h^3}{3}.$$

Therefore $\mathcal{M}_h^{\mathfrak{A}_x} = \frac{1}{12} h^2 \mathcal{S}_h^{\mathfrak{A}_x}$, and the proof is completed. \square

6.6. Numerical results. As mentioned before, our knowledge to construct a basis \mathfrak{B}^b for $V_{\#}^{\mathfrak{B},h}$ explicitly in 3D is lacking. Thus we only use the scheme option 4 for our numerical test.

EXAMPLE 6.19. Consider (5.1) on the domain $\Omega = (0, 1)^3$ with the exact solution $u(x, y, z) = \sin(2\pi x) \sin(2\pi y) \sin(2\pi z)$.

The numerical results for Example 6.19 given in Table 6.3 confirm our theoretical results.

h	Opt 4			
	$\ u - \bar{u}_h^{\mathfrak{A}}\ _{1,h}$	order	$\ u - \bar{u}_h^{\mathfrak{A}}\ _0$	order
1/8	1.505E-00	-	3.848E-02	-
1/16	7.550E-01	0.995	9.716E-03	1.986
1/32	3.777E-01	0.999	2.434E-03	1.997
1/64	1.889E-01	1.000	6.089E-04	1.999
1/128	9.443E-02	1.000	1.523E-04	2.000

TABLE 6.3
Numerical results for Example 6.19.

Acknowledgments. This research was supported in part by National Research Foundations (NRF-2017R1A2B3012506 and NRF-2015M3C4A7065662).

REFERENCES

- [1] A. Abdulle, E. Weinan, B. Engquist, and E. Vanden-Eijnden. The heterogeneous multiscale method. *Acta Numerica*, 21:1–87, 2012.
- [2] R. Altmann and C. Carstensen. P_1 -nonconforming finite elements on triangulations into triangles and quadrilaterals. *SIAM J. Numer. Anal.*, 50(2):418–438, 2012.
- [3] O. Axelsson. *Iterative solution methods*. Cambridge University Press, 1996.
- [4] I. Babuška. Homogenization approach in engineering. In *Computing methods in applied sciences and engineering*, pages 137–153. Springer, 1976.
- [5] I. Babuška, G. Caloz, and J. E. Osborn. Special finite element methods for a class of second order elliptic problems with rough coefficients. *SIAM J. Numer. Anal.*, 31(4):945–981, 1994.
- [6] P. Bochev and R. B. Lehoucq. On the finite element solution of the pure Neumann problem. *SIAM review*, 47(1):50–66, 2005.
- [7] S. L. Campbell and C. D. Meyer. *Generalized inverses of linear transformations*. SIAM, 2009.
- [8] C. Carstensen and J. Hu. A unifying theory of a posteriori error control for nonconforming finite element methods. *Numer. Math.*, 107(3):473–502, 2007.
- [9] W. E and B. Engquist. The heterogeneous multiscale methods. *Communications in Mathematical Sciences*, 1(1):87–132, 2003.
- [10] Y. Efendiev, J. Galvis, and T. Y. Hou. Generalized multiscale finite element methods (GMS-FEM). *J. Comp. Phys.*, 251:116–135, 2013.
- [11] Y. Efendiev, J. Galvis, G. Li, and M. Presho. Generalized multiscale finite element methods: Oversampling strategies. *International Journal for Multiscale Computational Engineering*, 12(6), 2014.
- [12] Y. Efendiev and T. Y. Hou. *Multiscale finite element methods: theory and applications*, volume 4. Springer Science & Business Media, 2009.

- [13] Y. Efendiev and A. Pankov. Numerical homogenization of nonlinear random parabolic operators. *Multiscale Modeling & Simulation*, 2(2):237–268, 2004.
- [14] B. Engquist and P. E. Souganidis. Asymptotic and numerical homogenization. *Acta Numerica*, 17:147–190, 2008.
- [15] X. Feng, I. Kim, H. Nam, and D. Sheen. Locally stabilized P_1 -nonconforming quadrilateral and hexahedral finite element methods for the Stokes equations. *J. Comput. Appl. Math.*, 236(5):714–727, 2011.
- [16] X. Feng, R. Li, Y. He, and D. Liu. P_1 -nonconforming quadrilateral finite volume methods for the semilinear elliptic equations. *J. Sci. Comput.*, 52(3):519–545, 2012.
- [17] T. Y. Hou and X.-H. Wu. A multiscale finite element method for elliptic problems in composite materials and porous media. *J. Comp. Phys.*, 134(1):169–189, 1997.
- [18] T. J. R. Hughes, G. R. Feijóo, L. Mazzei, and J.-B. Quinicy. The variational multiscale method—a paradigm for computational mechanics. *Comput. Methods Appl. Mech. Engrg.*, 166(1-2):3–24, 1998.
- [19] I. C. Ipsen and C. D. Meyer. The idea behind Krylov methods. *Amer. Math. Monthly*, pages 889–899, 1998.
- [20] P. Jenny, S. Lee, and H. Tchelepi. Multi-scale finite-volume method for elliptic problems in subsurface flow simulation. *J. Comp. Phys.*, 187(1):47–67, 2003.
- [21] L. Ju and J. Burkardt. MGMRES: Restarted GMRES solver for sparse linear systems. http://people.sc.fsu.edu/~jburkardt/f_src/mgmres/mgmres.html. [Online; revision on 28-Aug-2012].
- [22] E. F. Kaasschieter. Preconditioned conjugate gradients for solving singular systems. *J. Comput. Appl. Math.*, 24(1-2):265–275, 1988.
- [23] S. Kim, J. Yim, and D. Sheen. Stable cheapest nonconforming finite elements for the Stokes equations. *J. Comput. Appl. Math.*, 299:2–14, 2016.
- [24] R. Lim and D. Sheen. Nonconforming finite element method applied to the driven cavity problem. *Comm. Comput. Phys.*, 21(4):1012–1038, 2017.
- [25] H. Nam, H. J. Choi, C. Park, and D. Sheen. A cheapest nonconforming rectangular finite element for the stationary Stokes problem. *Comput. Methods Appl. Mech. Engrg.*, 257:77–86, 2013.
- [26] C. Park. *A study on locking phenomena in finite element methods*. PhD thesis, Department of Mathematics, Seoul National University, Seoul, Korea, 2002.
- [27] C. Park and D. Sheen. P_1 -nonconforming quadrilateral finite element methods for second-order elliptic problems. *SIAM J. Numer. Anal.*, 41(2):624–640, 2003.
- [28] D. Shi and L. Pei. Low order Crouzeix-Raviart type nonconforming finite element methods for approximating Maxwell’s equations. *Int. J. Numer. Anal. Model*, 5(3):373–385, 2008.
- [29] J. Yim, D. Sheen, and I. Sim. P_1 -nonconforming quadrilateral finite element space with periodic boundary conditions: Part II. Application to the nonconforming heterogeneous multiscale method. *this journal*. submitted.
- [30] N. Zhang, T.-T. Lu, and Y. Wei. Semi-convergence analysis of Uzawa methods for singular saddle point problems. *J. Comput. Appl. Math.*, 255:334–345, 2014.